ABSTRACT

JIANG, XIAO. A Tumor-on-a-chip for Studying Cancer Metastasis under Oxygen Gradient. (Under the direction of Dr. Michael Gamcsik.)

Cancer cells cultured in a low oxygen atmosphere which models hypoxic regions of tumors often show increased metastatic potential. Many studies concerning the relationship between cancer metastatic potential and oxidative stress have been done. The PDMS microfluidic device has the ability to create and maintain an oxygen gradient over its microchannels, thus is more and more commonly used to study oxygen gradient and cell metastasis. In this thesis, the design of a tumor-on-a-chip PDMS device is described. In this design, a gas channel layer sits directly above a cell channel layer. The gas channel layer enables the control of oxygen level and the creation of spatial heterogeneity of oxygen concentration in the media of the cell channel layer. The cell channel layer functions as an invasion assay with cells trespassing Matrigel blocked, capillary sized invasion channels. MCF7-0 and MDA-MB-231 cancer cells have been cultured in the device in order to determine the effect of oxygen content and an oxygen gradient on cell metastasis.

Tygon tubing is commonly used as a liquid delivery component in microfluidic device. In many microfluidic designs, cells are seeded and later perfused with growth media through the same Tygon tubing. However, this tubing could cause problems with cell viability. This thesis shows that cells trapped in this tubing can die from anoxia and release toxic factors into the perfusate. Experiments were performed to determine if lactic acid that is produced by mammalian cells during anaerobic respiration is produced in sufficient quantities in the anoxic cells in the Tygon tubing to have a negative effect on cell growth. The results show that a 20 mM lactic acid leads slower the growth of MDA-MB-231 cancer cells.

A Tumor-on-a-chip for Studying Cancer Metastasis under Oxygen Gradient

by
Xiao Jiang

A thesis submitted to the Graduate Faculty of
North Carolina State University
in partial fulfillment of the
requirements of the Degree of
Master of Science

Biomedical Engineering

Raleigh, North Carolina

2014

APPROVED BY:

Christine Grant	Gleen Walker

Michael Gamcsik
Chair of Advisory Committee

BIOGRAPHY

Xiao Jiang was born in Beijing, China, on July 15th, 1990. He attained his primary, middle and high school in Beijing. Later, he went to Zhejiang University in Hangzhou, China in August, 2008. He studied biology and got a Bachelor degree of biological Science at the College of Life Science in Zhejiang University in July, 2012. In the August of 2011, he came to North Carolina State University, U.S. as a student in 3+X program. After studying in the UNC/NCSU Joint Department of Biomedical Engineering for half a year, he was officially admitted as a graduate student pursuing the Master Degree of Biomedical Engineering at North Carolina State University.

In his undergraduate study, Xiao worked with Pro. Chengxin Fu from Zhejiang University. He studied systematic evolution of the plant in the family Smilacaceae, and the *in vitro* propagation of the plant *Tetrastigma hemsleyanum Diels et Gilg*. In his graduate study, Xiao worked with Dr. Michael Gamcsik from North Carolina State University. He studied cancer metastasis with microfluidic device. He participated in the fabrication of “Tumor-on-a-Chip” (toac) microfluidic device and successfully grew cells with this device. He also studied the use of Tygon tubing in this toac device and its effect on cell viability.

ACKNOWLEDGEMENTS

I would like to acknowledge everyone who has contributed to this research. I would like to thank my advisor, Dr. Gamcsik, for the opportunity to work under his tutelage, and further for his patience, mentorship, kindness and guidance, without which I could not have completed this work. I would also like to thank Dr. Walker, for his constant instruction and encouragement. I would like to thank Dr. Miguel Acosta for working with me together on this research, giving me a lot of encouragements and good ideas. I would also like to thank Eason Huang, for giving me instruction of this research. I would also like to thank Ms. Staphaine Tetter, Ms. Vindhya Kunduru, Dr. Rex Jeffries and everyone else that has helped me in my graduate study. I would also like to thank my committee for your time and effort in ensuring I could succeed in this endeavor.

I would also like to thank my friends who came with me here from China, for their helps without which I would have a hard time to adapt the life here. Finally, I must acknowledge my parents who have gave birth to me, raised me as I am, always being considerate and supported me for education.

LIST OF CONTENTS

LIST OF FIGURES

Chapter 1. Literature Review

1.1 Breast Cancer

Breast cancer originates in breast tissue, which is composed of the milk producing lobules, the ducts connecting lobules to the nipple, and fatty, connective and lymphatic tissue[8]. Breast cancer constitutes many subtypes with diverse malignant grade[97]. Most breast cancers begin in the cells of lobules or the ducts. Those that stay within the lobules or ducts are non-invasive, also called carcinoma in situ, and those that spread into normal tissue are invasive cancers[126]. The progression of breast cancer can be classified by how far it has spread, from stage 0, non-invasive breast cancer to stage IV, invasive breast cancer that has spread beyond breast tissue and nearby lymph node to distant organs, such as lung, bone and brain[163]. Breast cancer is the most common malignancy among women [122,168]. According to the estimate of the American Cancer Society, the number of new cases of invasive breast cancer in America in the year of 2011 was 230,480 and the number of new cases of in situ breast cancer was 57,650[8]. In addition to its pervasiveness, breast cancer is also highly invasive. Even though the earlier detection and the use of systemic adjuvant treatment have increased the survival rates, still half of the patients develop metastases[122]. Most of the patients who die of breast cancer are not killed by the primary tumor, but are killed by its metastasis to distant organs[24,182]. Studies have shown that the increased lymph node involvement has a negative effect on percentage of relative survival, and is independent of tumor size[41]. Though lymph node involvement has been a prognostic criterion indicative of worse outcome and aggressive disease, it is notable that lymph node metastasis would not necessarily lead to distant metastasis[98]. Commonly, breast cancers metastasize to lung, liver, bone and brain[85].

1.2 Hypoxia in Tumors

Hypoxia is the reduction of oxygen tension below the normal level for a specific tissue caused by the imbalance between oxygen delivery and oxygen consumption[118,122]. Hypoxia may occur when a tumor outgrows its blood supply. Though tumors usually induce blood vessel growth (angiogenesis) to support their expansion, the blood vessels developed in tumors are often abnormal functionally and structurally[120]. The blood vessels in a solid tumor are not evenly distributed, and the center of the tumor often has less vascular density[153]. Also, some tumor microvessels contain very few to no red blood cells[54]. Thus, solid tumors often consist of regions of chronic hypoxia, where the oxygen tension is limited by diffusion, and regions of intermittent hypoxia, where the aberrant blood vessel shut off temporally followed by reperfusion[97,120]. The portion of intermittent hypoxia in tumor is significant, and there is study showing that up to 20% cells in human cervical squamous cell carcinoma tumors experience intermittent hypoxia over periods of several hours[15]. The oxygen tensions of several cancer types have been measured, showing values between 0~20 mmHg in tumor tissues, which are significantly lower than 24~66 mmHg, which is measured from adjacent normal tissues[25,165,173]. Dewhirst in 1998 measured the pO_2 in mouse tumors. The results suggest that the temporal fluctuation in pO_2 is a common phenomenon in tumors, and the hypoxia/re-oxygenation turnover occurs at a rate of 4-7 events per hour [53]. More and more studies have been done to elucidate the periodicity of hypoxia, and the results suggest that there exist two frames (Figure 1.1). There are fluctuations in pO_2 of one to three cycles per hour[36,54,110], and a more prolonged time scale where fluctuations happen on a day to day basis[28,161].

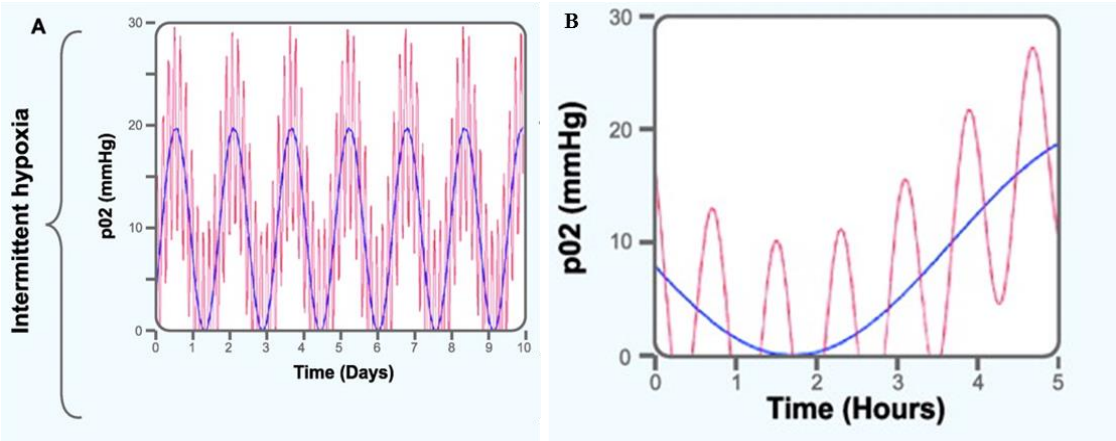

Figure 1.1 Periodicity of intermittent hypoxia. A: fluctuations over days occur as a result of angiogenesis and remodeling of tumor vasculature (blue line). B: fluctuations on a time scale of one to three times per hour occur as a result of fluctuations in red cell flux in vascular networks (red line). Figure is derived from Ref.55.

Tumor hypoxia has known to be a poor prognostic indicator, predictive of increased risk of metastatic disease and reduced survival[104]. Chronic/intermittent hypoxia has various effects on many aspects of carcinogenesis. Hypoxia especially intermittent hypoxia can activate HIF and stabilize HIF, as explained in next section. Also, intermittent hypoxia would raise the level of reactive oxygen species (ROS) in tumor cells, and ROS may participate in the stabilization of HIF[89]. Other studies also show that intermittent hypoxia causes increased oxidative stress, and this leads to more genomic instability[104,105].There are several reports on the relationship between hypoxia and metastasis[32,33,49]. De Jaeger in 2001 showed that hypoxia increased the metastatic potential of KHT-C fibrosarcoma in rodent models[49]. Furthermore, Cairns in 2001 showed that cycling hypoxia treated tumor cells have larger metastatic potential than those treated by chronic hypoxia[32,33]. That intermittent hypoxia tumor cells have larger metastatic potential than chronic hypoxia tumor cells has also been proved by Rofstad in 2007[147]. Yamaura in 1979 observed tumor regrowth after radiotherapy predominantly at the tumor periphery. He suggested that the radio-resistance of

the tumor cells at the periphery might be related to transient hypoxia, because that temporary vascular stasis in the tumor periphery has been occasionally observed before the irradiation[185]. The radio-resistance effect of cycling hypoxia on tumor cells has been proved later by Hsieh. This study showed that U87 glioma cells treated with cycling hypoxia have higher levels of HIF-1 and are more radio-resistant than those treated with uninterrupted hypoxia[89]. In conclusion, hypoxia especially intermittent hypoxia increases the metastatic potential and therapy resistance of tumor cells. It also affects many other processes of cancer development through HIF and ROS and other mechanisms. Thus, it is important to study the effect of chronic/intermittent hypoxia on tumor cells.

1.3 Hypoxia Inducible Factors

There are many defensive responses that tumor cells use to fight hypoxic stress. Tumor cells may stop proliferation, reduce energy consumption, rely more on glycolysis and release survival and proangiogenic factors[120]. Many of these responses are regulated by a sequence specific DNA binding transcription factor, Hypoxia Inducible Factor (HIF), which has been recognized as a key modulator of transcriptional response to hypoxic stress and also plays a key role in many crucial aspects of cancer biology[120,154]. HIF-1 has been found in all metazoan species analyzed to date[154]. HIFs are heterodimers consist of a HIF α subunit and a HIF β subunit, the former of which is regulated by oxygen and the latter is stably transcribed.

The basic model to illuminate how HIF responses to cellular oxygen availability change is through hydroxylation of both HIF α and factor inhibiting HIF1 α (FIH1)[120,154]. The hydroxylation of HIF α is mediated by prolyl hydroxylase domain enzymes (PHDs), which are 2-oxoglutarate- and iron- dependent dioxygenases. With oxygen as a direct substrate, PHDs are able to sense the cellular oxygen level, thus

couple the HIF activity with oxygen availability. In normoxic conditions, PHDs hydroxylate HIF at conservative proline residues, thus mark it for proteosomal destruction by the von Hippel-Lindau protein (pVHL) complex; in hypoxic conditions, PHDs' activity is diminished and HIF α stabilized[95,120]. Studies have shown that tumor cell mitochondria produce reactive oxygen species (ROS) in severe oxygen deprivation. ROS could also antagonize PHD activity by oxidizing the Fe(II) in the hydroxylases' catalytic center[79,106].

In hypoxic conditions, without hydroxylation, HIF α is stabilized, thus it is able to dimerize with HIFβ and relocate into nuclei. Dimerization is necessary to enable binding to the specific hypoxia response elements (HRE) in a gene's promoter region. The HIF dimer interacts with its coactivators and start transcription of the targeted gene[106]. HIF targets about 100~200 genes that protect cells from low O_2 stress[95]. In hypoxic conditions, cells have limited oxygen and cannot utilize the tricarboxylic acid cycle and oxidative phosphorylation pathway to metabolize glucose and to generate energy. Along with other factors such as proto-oncogene c-Myc, HIF1 α guides the metabolic shift from the tricarboxylic acid cycle to glycolysis. These effects directly enhance glycolysis and block glycolytic end products from entering the mitochondria[76,120]. Another effect of HIF on tumor cell survival is reducing reactive oxygen species (ROS), which has been observed to be elevated in many types of cancer especially under hypoxia [7,98]. Under hypoxia, ROS are suggested to be generated at the site of complex III of the electron transport chain, through unknown mechanisms[79]. Though ROS are believed to play roles in many of the signal mechanisms for tumor progression, it can damage DNA and RNA and oxidize polyunsaturated fatty acids as well as amino acid residues in proteins. Though many studies have been done, we still don't know the

whole picture of how HIF, ROS and other angiogenic factors interact in hypoxic tumor cells, or the roles they play in cancer metastasis.

1.4 Cancer Metastasis

Nearly 90% of cancer associated mortality is caused by metastatic disease. Cancer metastasis has always been under close scrutiny, yet it remains the most poorly understood part of cancer pathology. Metastatic dissemination of cancer contains the following main steps. The first is intravasation, in which cancer cells invade the surrounding tissue and enters a blood or lymphatic vessel. Secondly, carried by the circulatory system (primarily blood vessels), metastatic cancer cells are arrested by the size restriction of the small capillary at distant tissues. The next step is extravasation, in which the trapped cancer cells exit from the bloodstream to the parenchyma of the tissue. Tumor cell extravasation could happen via diverse mechanisms. After being trapped in the blood vessel, adherent tumor cells may invade through the intracellular junction of endothelial cells (paracellular route) or else, they may penetrate through the endothelial cell body (transcellular route)[98,109]. Some tumor cells secrete products that stimulate endothelial cell retraction, whereas other tumor cells proliferate within the vessel lumen and finally rupture the vessel itself[5,87,109]. Recent studies have shown that a distinct population of $CD11b^+$ macrophages may mediate the extravasation process[140]. Finally, the extravasated cancer cells need to survive at the new site, proliferate and form a new macroscopic secondary tumor[34]. After gaining access to the underlying tissue parenchyma, tumor cells establish reciprocal signaling networks with stromal cells to promote their growth[109]. To meet the increasing metabolic demands for unrestrained cell division, tumor cells synthesize proangiogenic signals that orchestrate microvascular endothelial cells to form new vascular networks[109].

It has been long recognized that cancer metastasis is intrinsically an ineffective process, in which only less than 0.01% of circulating tumor cells finally succeed in forming secondary tumors[60,109]. The first steps of metastasis—arrest in tissue and extravasation appears to occur with high efficiency, yet the following step —the outgrowth to form macroscopic metastasis was considered to be the limiting step of the process[31,35,119]. The temporal duration of the metastatic process could be as long as decades. Metastatic cancer cells could enter a dormant state, thus metastasis may relapse years after the primary tumor has been removed. Recently, Yachida *et al*. performed a quantitative analysis for the timing of the genetic evolution of pancreatic cancer. Their result indicated that there is at least a decade between the occurrence of the initiating mutation and the birth of the parental, non-metastatic founder cell. At least five more years are required for the development of metastatic ability and patients die an average of two years thereafter[184].

1.5 Cancer Metastasis Models

In 1965, Leighton hypothesized that metastases arise from definite genetically determined subpopulations in primary tumors[112,178]. By injecting B16 melanoma cells intravenously into mouse, Fidler in 1973 found that metastatic tumor cells have greater metastatic potential than the primary tumor cells from which the metastasis arises[61]. In 1977, Fidler *et al*. also observed variant metastatic potentials from intravenously injecting *in vitro* clones of a parental culture of murine malignant melanoma cells into mouse[62]. These observations support the theory that tumor cells are heterogeneous, and in any tumor there exist subpopulations which are more apt to generate secondary metastasis. Moreover, Fidler further suggested that these subpopulations evolve during later stage of tumorigenesis, in which rare cells from low metastatic potential primary tumor cells acquire metastatic capacity through additional somatic mutations[62,178]. There

is also a spontaneous metastasis model suggested later, where all tumor cells have the ability to form metastasis[179]. Except for the spontaneous model, different hypotheses have been put forward to elucidate the discrepancies observed in experiments concerning the presumed selective nature of the metastatic phenotype[71,72,81,99,100,115,116,151].

The research concerning cancer stem cells allows us to speculate about a new model of metastatic process. Since stem cells already possess the capability of self-renewal and differentiation, it is likely that cancer stem cells arise from malignant mutation of normal stem cells rather than from differentiated cells within the organ that undergoes de-differentiation and adapt a stem cell phenotype. Furthermore, normal stem cells are the longest lived cell, thus believed to have a greater likelihood of accumulating mutations[90]. Based on the expression of estrogen receptor, Dontu proposed a stem cell model of mammary carcinogenesis, which suggested that mutations occurring in differentiated progenitor cells might form a non-metastatic good prognosis breast carcinoma, whereas mutations occurring in stem cells might lead to breast stem cell that generates poor-prognosis tumors[56,178].

More and more evidence has shown that rather than developing alone, cancer cells interact with their environment in tumorigenesis[11,19,134,156,159,166]. It is likely that during tumor progression, there is a selection of specific phenotypes in cells composing the tumor microenvironment that co-evolves with the primary tumor[134]. Carcinoma cells live in a complex microenvironment composed of the extracellular matrix (ECM), diffusible growth factors and cytokines, and a variety of non-epithelial cell types, including vasculature associated cells (endothelial cells, pericytes and smooth muscle cells), inflammatory cells

(lymphocytes, macrophages and mast cells), and fibroblasts[18]. The structural scaffold in this microenvironment is ECM, which is produced by stromal fibroblasts and epithelial cells. The ECM serves as the support that separates fibroblasts and epithelial cells, and also the medium that delivers nutrients and various signaling molecules[18,19]. Under normal conditions, epithelial cells form intact, polymerized sheets, and communicate with their neighboring cells through different types of cell junctions and with other types of cells through signaling molecules. These communications between the epithelial cells themselves and the fibroblasts and other types of cells create a dynamic equilibrium where the cells maintain a normal, differentiated phenotype[19], and can even keep epithelial cells with oncogenic mutations at bay[51,65]. Carcinoma cells (believed to evolve from pre-cancerous epithelial cells that have acquired multiple genetic mutations[174], however, can gradually break the equilibrium by releasing signals that induce angiogenesis, ECM alteration, fibroblast proliferation and inflammatory cell recruitment[18]. This cancer modified stroma then creates a context that promotes tumor growth, immigration, and protects it from immune attack[19]. It has been suggested that tumor expansion and the progression to advanced stages of the disease requires the co-evolution of both cancer cells and cancer stroma[156], as their association changes along with the malignancy[19]. For example inflammatory response associated with tissues wounding can produce tumors or accelerate the development of epithelial cancers[11,19]. In the activation of tumorigenesis, the ECM is remodeled by mesenchymal cells such as myofibroblasts. This process is believed to promote carcinoma progression through a variety of mechanisms[159, 166]. The carcinoma-associated fibroblasts (CAFs) can affect tumor progression in an autocrine or/and paracrine manner[18]. CAFs express various growth factors, cytokines and ECM proteins, and many of these factors and proteins are related to carcinogenesis[1,9,22,148,149]. CAFs can also induce epithelial-mesenchymal transition (EMT)[52,165], stimulate myrofibroblasts

generation[50], produce autocrine mitogens[27,93], suppress $CD^{+}8$ T and NK cells[67,77,167], promote distant metastasis[63], and affect many other aspects in tumorigenesis[173]. Karnoub in 2007 has shown that the mesenchymal stem cells in CAFs could enhance breast cancer metastatic potential in a paracrine fashion[9].

Inflammation is another critical component of tumor progression. Tumor cells utilize some of the signaling molecules from the innate immune system to provoke its growth and metastasis[45]. Malignant cells can dodge immune surveillance by reducing their own endogenous tumor antigen[13] or by modulating the inhibitory natural killer receptor function thus down-regulating the lytic activity of tumor-specific cytotoxic T lymphocytes[19,73]. Studies regarding squamous epithelial carcinoma[44,46], pancreatic carcinoma[17], and mammary tumors[114] have shown that inflammatory cells such as mast cells promote tumorigenesis by inducing MMPs production[19,45,57,66]. Matrix metalloproteinases (MMPs) are zinc-dependent endopeptidases that break down the ECM, thereby promoting the invasion of metastatic cancer cells and bone marrow derived cells into the tissue. The invasion of these cells is a key process to metastasis.

1.6 Cancer Stem Cells

A stem cell is characterized by its ability to self-renew and to give rise to different types of cells. As early as 1937, Furth has shown that a single tumor cell can initiate a tumor in a new recipient mouse[69]. It has been long documented that most tumors have a clonal (single cell) origin[58,59,120,128] and contain cancer cells with heterogeneous phenotypes[5,84]. Though heterogeneity in tumors could arise from mutations during tumor progression, the variable expression of normal differentiation markers by cancer cells suggests that this heterogeneity might also come from aberrant differentiation[144]. Moreover, many studies have shown that

only a small proportion of cancer cells in a tumor have the ability to proliferate in culture or give rise to new tumors in mouse models[20,58,59,128,144]. By injecting thymidine-3 H into mouse which bears well differentiated squamous cell carcinoma, Pierce in 1971 showed that the radiolabel appeared first in undifferentiated areas and differentiated area failed to form tumors in compatible hosts[137,138]. Thus, it is likely that there exist tumorigenic cancer cells which can indefinitely proliferate and produce phenotypically diverse progeny cancer cells. These cancer cells undergo processes analogous to self-renewal and differentiation of normal stem cells[144]. Similar to the process in which normal stem cells differentiate into phenotypically diverse progeny with limited proliferative potential, it is argued that cancer stem cells undergo epigenetic changes, giving rise to phenotypically diverse nontumorigenic cancer cells that compose the bulk of cells in a tumor[155]. Recent work has also suggested that cancer stem cells (CSCs) explains the tumor's therapy resistance. CSCs isolated from tumors originating in the breast and other tissues exhibit resistance to chemotherapy and radiation[96,136, 150].

From the early nineties, substantial evidence supports the existence of CSCs. Studies have shown that cancer stem cells are rare[20,43,111]. Many surface markers have been used to characterize cancer stem cells[3,48,74,129,145,159]. In the studies that characterize CSCs, the cancer cells sorted by CSC markers could initiate secondary tumors with small cell numbers. The transplanted tumors were able to reproduce at least some of the heterogeneity of the original tumors[43]. However, there are also a lot of caveats to the CSC hypothesis. First of all, most of the studies to identify CSC are based on the difference of only two or three surface markers. It has not been determined whether there is other heterogeneity presents in primary tumor which has not been reproduced in transplanted tumors. Furthermore, some CSC markers such as CD34 and

CD38 are first extensively validated in the identification of normal hematopoietic stem cells, thus fitted the identification of leukemia stem cells[20,111]. These markers however, are not well characterized in most tissues that develop tumors, and some of them for instance CD133 has been revealed to be widely expressed in many organs[157]. As a result, they may not be as effective in CSC characterization[142,155]. In conclusion, the cancer stem cell model has only been carefully tested on a small subset of tumors. There is still a lot of work to be done to explore the CSC hypothesis. It seems that not all kinds of tumors would follow the cancer stem cell model, or the character required to distinguish cancer stem cell in some tumors (such as melanoma) has not been identified.

1.7 Oxidative Stress and Cancer Metastasis

As mentioned above, reactive oxygen species (ROS) and reactive nitrogen species (RNS) had been shown to modulate many processes of cancer development[80,181]. There are studies as early as 1984 showing that exposing mouse fibroblasts to ROS leads to malignant transformation[179]. Also, John in 2004 has found that mtDNA mutations that affect mitochondrial functions and inhibit oxidative phosphorylation can increase ROS, which later contributes to tumorigenicity in prostate cancer[187]. ROS could cause structural alterations in DNA, for example base pair mutations, rearrangements, deletions, insertions and sequence amplification[80]. This could be cancerogenic when the mutation leads to the inactivation or loss of the second wild-type allele of a mutated proto-oncogene or tumor-suppressor gene[179,180]. Moreover, ROS could affect cytoplasmic and nuclear signal transduction pathways[29,30 ,152]. Evidence suggests that transformed cells use ROS signals to drive proliferation and other events required for tumor progression[135]. Low levels of ROS play an important role in normal cell proliferation[29]. Gupta *et al.* in 1999 has suggested

that transcription factors which regulate several genes in carcinogenesis such as NF- κ B and AP-1and mitogen-activated protein kinases (MAPKs) are potential targets involved in ROS-mediated mitogenic signaling[78]. He also suggested that elevated ROS levels implicate the activation of cell proliferation and differentiation related molecules such as Erk-1/2 and p38 MAP kinase in the malignant progression of mouse keratinocytes[78]. Furthermore, ROS levels are elevated in cells stimulated with growth factors such as EGF and PDGF[10], and the scavenging of extracellular H_2O_2 by catalase inhibits the proliferation of Her-2/neu-transformed Rat-1 fibroblasts[14,139]. However, the effects of ROS on cells can vary, and is dependent on the amount of ROS and the type of cells. Cells exposed to ROS can show increased proliferation, halted cell cycle, senescence, apoptosis or necrosis[80]. Moderate levels of ROS tend to promote apoptosis in normal cells. ROS could increase p53 activity and trigger senescence. Higher p53 activity can cause ROS production by several mechanisms, and these ROS might contribute to the cytostatic and pro-apoptotic effect of p53[16,80]. Also as mentioned above, most chemo- and radiotherapy depends on the elevation of ROS to kill cancer cells.

ROS have also been suggested to play roles in cancer metastasis. Kundu in 1995 suggested that oxidative stress could affect tumor cells' attachment to laminin and fibronectin, and oxidative treating tumor cells before injection enhances the lung colony formation in mouse model[107]. Many ROS and nitric oxide donors stimulate the expression and activation of several MMPs[125,143]. MMPs as mentioned above, degrade ECM proteins thus play key roles in cancer metastasis. Cheng in 2004 suggested that ROS-sensitive signaling cascades participate in the mediation of transendothelial migration step in melanoma cells intravasation[39]. ROS could mediate a process that could damage the integrity of the endothelium and

promote cancer cell invasion[172]. Moreover, studies concerning lysyl oxidase (LOX) have shown that LOX facilitates migration and cell-matrix adhesion formation in invasive breast cancer cells through a hydrogen peroxide–mediated mechanism[133]. Furthermore, ROS participate in many growth factor signal pathways which stimulate proliferation, migration, and tube formation of endothelial cells[101,169]. In a study concerning the metastasis of cancer cells exposed to hepatic ischemia-reperfusion, ROS and RNS have been shown to kill weakly metastasis cancer cells. This may help to select more metastatic cancer cells in those invading through the tumor stroma and entering the oxygen rich circulatory system[94].

It is well known that a large amount of ROS are generated during reperfusion of post-ischemic tissue[203]. As a result, ROS are also present in a hypoxic solid tumor, especially in the intermittent hypoxia region. What's more, ROS levels could also be elevated when metastatic cancer cells are exposed to oxidative stress as they migrated into the oxygen rich blood vasculature[6]. Along with the HIF mentioned in section 1.3, ROS are suggested to cooperate in cancerogenic transformation, cancer cell proliferation, angiogenesis, the generation and maintenance of cancer stem cells and cancer cell metastasis.

1.8 Models to Study Oxidative Stress in Tumor

Since oxidative stress plays an important role in tumor development, a large amount of research has been done to address chronic/intermittent hypoxia in tumor. The methods to control the oxygen concentration exposed to cells vary in these studies. Many of them study the link between hypoxia/acute hypoxia and tumor metastatic potential by putting tumor bearing mice into gas chambers and treating them with sections of hypoxia/re-oxygenation[32,33]. For example, Carins in 2001 introduced acute hypoxia by treating tumor

bearing mice with 12 cycles of 10-minute exposure to 5–7% O_2; balance N_2/10 minute air once per day, 7 days per week[32]. Though they have got significant results which suggest an increased number of spontaneous microscopic metastases in the mice treated with acute hypoxia, it is arguable whether the tumors in mice are exposed to the same periodic oxygen level changes as their hosts do. Also, hypoxia would have systemic effects on the hosts, for example an overall rise in lactic acid levels, and these would also affect the metastatic result. It is hard to sort this effect out of the effect on tumor cells. Other methods that introduce oxygen level changes *in vivo* are based on cutting the blood supply of tumors. Parkins in 1995 studied ischemic/reperfusion injury on tumors by using a metal D clamp. The clamp tightens across the skins surrounding the superficial tumor thus makes the tumor hypoxic[131]. Toshikazu in 1994 infused a transient embolic agent (degradable starch microspheres, DSMs) into tumor vessels to study the anti-tumor effect of ischemic/reperfusion injury. The DSMs occluded the tumor vessels for 40 minutes[186]. However, it is hard to introduce cycling hypoxia with short period with these *in vivo* methods, and it is also hard to know whether the hypoxic levels introduced by these methods are relevant to those observed *in vivo*. Moreover, the clamp and embolism approach are not suitable to study cancer metastasis, for they disrupt the important intravasation process. These *in vivo* approaches also fail to control hypoxia levels, periodicity and spatial variation.

Except for the *in vivo* studies mentioned above, a lot of *in vitro* studies also involve the controlling of oxygen content in atmospheres above cultured tumor cells. One traditional method is to put cells directly into conventional gas variable incubators with atmosphere created by a certain gas mixture. This method is

still commonly used. For example, Dai in 2011 cultured prostate cancer cells in a modular incubator chamber flushed with certain gas mixture (hypoxic and normoxic) to test their motility by a "wound healing" assay. The result shows that hypoxia increases the cell's motility[47]. Patrick in 2008 incubated Transwell chambers with chronic hypoxia by controlling the oxygen concentration in the incubator to test the invasive potential of HT1080 fibrosarcoma and MDA MB231 carcinoma cells[164]. Hsieh in 2012 plated Transwell invasion chambers with glioblastoma cells, and further put the Transwell chamber into gas chamber infused with cycling hypoxia gas mixture to show that cycling hypoxia increases glioblastoma invasion via ROS regulated pathway[88]. The cycling hypoxia used in Hsieh's study has a period of 4 hours. However, cycling hypoxia in a solid tumor could have period from minutes to days[23], and it takes hours for the oxygen concentration of the media in Transwell chamber to equilibrate with that of the atmosphere[4]. As a result, though it is easy to create chronic hypoxia with accurate concentration control by placing traditional cell culture flask or Transwell invasion chamber into a gas chamber, it is hard to create cycling hypoxia with short periods of time. Nor is it easy to create and maintain a spatial variation of oxygen concentration with these macro culture approaches.

Due to the high gas permeability of PDMS and the small diffusion distance, many recent studies used PDMS microfluidic devices to study the effect of hypoxia and oxygen concentration on tumor cells. A microfluidic device can be identified by the fact that it has one or more channels with at least one dimension less than 1 mm. The small diffusion distance of micro-scale device enables the realization of fast reversibility between hypoxia and re-oxygenation. The flow in the microhannels is laminar rather than chaotic as in the macro-scale channels, and this makes it possible to maintain a gradient in the

microchannels. Also, with PDMS device, it is possible to create an oxygen gradient over tens of microns distance, which conventional gas variable incubators cannot[68]. These spatial gradients are to be expected in a tumor cell migrating into a blood vessel. For example, Oppegard in 2009 developed a microfabricated insert to control oxygen tension temporally (in minutes) and spatially (in millimetres) in a well plate commonly used for cell cultures[130]. Raymond in 2009 controlled the oxygen gradient in microchannels by controlling the gas mixture in the proximal gas channels. The oxygen molecule in

gas channels diffuses through PDMS membrane and equilibrates with the dissolved oxygen concentration in the microchannels filled with media (Figure 1.2) [108]. Joe in 2010 developed an open well cell culture chamber with a PDMS substrate. This design allows the delivery of microgradients of oxygen concentration without exposing cells to mechanical stresses or reducing culture volumes inside microfluidic culture chambers[117]. In conclusion, there are more and more *in vitro* hypoxia tumor models developed with PDMS microfluidic device. These devices have the ability to introduce small scale temporal and spatial control of oxygen concentration on cells, thus has advantages over the traditional approaches such as conventional gas variable incubator.

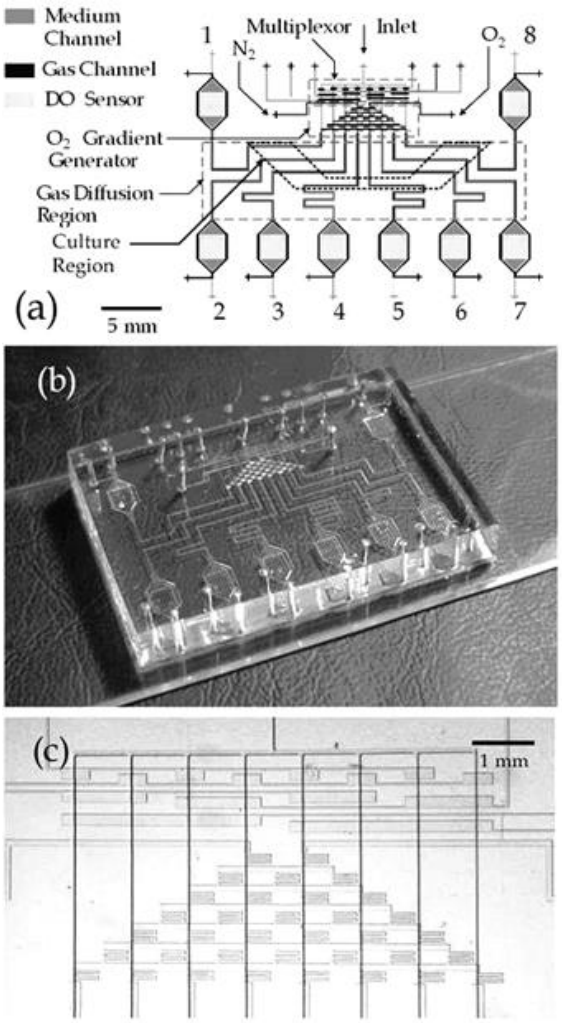

Figure 1.2 Raymond's device with oxygen diffusion layer. (a) Schematic diagram of microfluidic oxygenator. The device consists of two PDMS layers (gas and medium) that contain molded microchannels. The multiplexor and O2 gradient generator are contained in the gas layer, while the DO sensors are contained in the medium channels. (b) Fabricated microfluidic oxygenator. (c) Micrograph of the multiplexor and the oxygen concentration gradient generator; Figure is derived from Ref.108

1.9 Conventional and Microfluidic Cancer Cell Invasion Assay

As mentioned above, the PDMS microfluidic device enables us to create and maintain temporal and spatial variation changes of oxygen concentration. The next thing to be done is to combine a micro-scale, PDMS based invasion assay with the oxygen delivery part. Conventional cell migration assays consist of Boyden chamber and the "wound healing" assay. The wound-healing assay is simple, inexpensive, and one of the

earliest developed methods to study directional cell migration *in vitro*[146]. Basically, a wound healing assay is first creating a "wound" in a cell monolayer, then monitoring how long it takes for the cells to close the wound. This assay has been adapted into a microfluidic system. Huang in 2011designed a microfluidic device which can partially digest a confluent cell sheet using parallel laminar flows in the presence of protease trypsin to quantify the effect of ethanol on MCF-7 human breast cancer cells[91]. Also, a similar device has been used by Andries in 2010 to study endothelial cell migration[171]. However, neither is the wound healing assay a quantitative approach, nor is it suitable to mimic the process in which tumor cells invade through the basement membrane.

The basement membrane is a thin continuous sheet which separates epithelial tissues from adjacent stroma and forms barrier that blocks the passage of cells and macro molecules[2]. Tumor cell invasion of basement membranes is a crucial step in cancer metastasis[2]. A type of Boyden chamber, a commercial product called a Transwell invasion chamber, contains two medium-filled compartments separated by a microporous membrane. Cells are placed in the upper compartment and are allowed to migrate through the porous membrane to the lower compartment[38].By staining and counting the cells that have traversed the membrane and grown on the lower surface, Transwell chambers can achieve a quantitative assessment of cancer cell migration. Albin in 1987 coated the porous membrane with Matrigel as a mock basement membrane to test the invasive potential of tumor cells[2]. This design has been widely used to assess cell aggressiveness, and the Matrigel coated Transwell chamber is also commercially available[38]. However, these Transwell chambers also have its drawbacks. Firstly, the counting step is laborious. Moreover, due to the large surface area of the insert membrane, only a number of fields can be chosen from the whole insert

membrane area and counted. Since the cells placed on the upper surface of the insert membrane do not spread uniformly, the cells traversing the pores and growing on the lower surface would also be non-uniformly distributed. This non-homogeneity could bring errors to the counting result[113,124,160].Furthermore, the cells which have traversed the insert membrane could detach from it into the bottom of the well. These cells are mostly neglected during the counting step[160].

The idea of the Transwell chamber has been adapted into many microfluidic designs to study cancer metastasis[37 ,42]. Chung in 2009 developed a microfluidic platform to evaluate and quantify capillary growth and endothelial cell migration. In this design, side channels connected to the main channels are blocked with collagen, and the cells growing in the main channel migrate into these collagen scaffolds[42]. Chaw in 2007 developed a microfluidic device with micro gaps connected to two micro-channels. Cells cultured in one channel migrate through the capillary-like micro gaps to the other channel[37]. Another similar device is developed by Irimia in 2007. In this design two main channels are connected by many microchannels as migration paths[92].The side channels and micro gaps of these designs are similar to the pores of the insert membrane of Transwell chamber. Nevertheless, these microfluidic devices have advantages over Transwell chamber. The cells in the transparent PDMS device can be accurately counted, thus the instability and inaccuracy problem of Transwell chamber qualification is solved. Moreover, microfluidic device has many advantages over macro culture device, for example the small requirement of samples, high throughput, low cost, accurate environment control, versatility in design, and potential for parallel operation and for integration with other miniaturized devices[158]. Many microfluidic devices with other designs have also been developed[40,177]. For example, Cheng in 2007 developed a microfluidic device made with hydrogel.

This device allows cells migrate freely from the hydrogel based channels without the restriction of a pre-set path[40].

1.10 Lactic Acid and Cancer Metastasis

Measurement of tumor pH reveals that the pH of tumor is about 0.5 lower than that of normal tissue[127].The acidity in tumor has been suggested to be caused by the Warburg effect[127]. A high rate of aerobic glycolysis results in the production of large amounts of lactic acid compared to normal tissue[127]. The Warburg effect is defined by a shift in energy production from oxidative phosphorylation to glycolysis in tumor cells[70]. This effect has been suggested to be advantageous to tumor cells in its microenvironment and also a fundamental property of tumor cells[70,102]. However, a new model about tumor metabolism——"the reverse Warburg effect", has been put forward by Pavlides *et al* in 2009. Pavlides' group suggested that epithelial cancer cells induce Warburg effect in neighboring stromal fibroblast cells. The stromal cells secrete lactate and pyruvate into the tumor stroma, then epithelial cancer cells take up this energy-rich metabolites and use them in the mitochondrial TCA cycle, thereby promoting efficient energy production[132]. Bonuccelli *et al* in 2010 showed that 3-hydroxy-butyrate (a ketone body of the end product of aerobic glycolysis) increases tumor growth by ~2.5-fold[21].

Lactic acid has been suggested to be a key player in tumor metabolism[86]. A recent study suggests that lactic acid functions as an intrinsic inflammatory mediator that promote chronic inflammation in tumor microenvironments[183]. Also, the low pH in tumor microenvironment results in a reduction of cytotoxic T-cell function, thus helps tumor to escape immune surveillance[64]. Moreover, many studies suggest that

lactic acid could enhance tumor cell motility[21,75] and triggers VEGF production by endothelial cells, thus promoting angiogenesis[12]. Also, clinical results show that the content of lactic acid is in negative correlation with disease-free patient survival[176], and is in positive correlation with the incidence of metastasis[175, 187].

Chapter 2. Long Term Cell Culture in PDMS Microfluidic Device and the Use of Tygon® Tubing in the Media Deliver System

Tygon tubing is commonly used as a liquid delivery component in microfluidic devices. In many microfluidic designs, cells are seeded and later perfused with growth media through the same Tygon tubing. However, this tubing could cause problems with cell viability. The experiments outlined in this chapter show that cells trapped in this tubing can die from anoxia and release toxic factors into the perfusate. Experiments were performed to determine if lactic acid that is produced by mammalian cells during anaerobic respiration is produced in sufficient quantities in the anoxic cells in the Tygon tubing to have a negative effect on cell growth. The results show that a 20 mM lactic acid leads to slower growth of MDA-MB-231 cancer cells.

2.1 Introduction

Culturing cells in microfluidic systems enables us to more accurately control the environmental cues[4]. However, there are a lot of challenges for long-term cell culture in microfluidic devices. For example, the geometry, the method of nutrient delivery, the avoidance of air bubbles, the control of flow rate, the substrate treatment for cell attachment (if culturing attached cells), the prevention of media evaporation etc.[2,4,7]. Because microfluidic chambers only hold a small volume of media, the question of whether cells could get enough nutrients between media replenishments should be considered in the design of microfluidic device. Air bubbles can accumulate in long term cell culture and their surface tension makes them stick to the inner surface of micro-scale channels. The presence of air bubbles not only blocks the fluidic path and distorts the flow, but also can damage the cells at the liquid-gas interface[9]. Furthermore,

the substrate commonly used in the fabrication of microfluidic devices is glass, which does not support cell attachment without coating with serum or fibronectin.

Our project studied another challenging aspect of microfluidic cell culture. In our project, three different methods to deliver cell growth media from a reservoir to the chip have been tested (Figure 2.1). In the original design, the media was withdrawn from an off chip Petri dish reservoir through a short length of Tygon tubing to the PDMS chip (Figure 2.1c). This same short length of Tygon tubing was used initially for cell seeding. The tubing is filled with cells in growth media for delivery to the chip. Once the cells fill the microchannel, the tubing is clamped for 4 hours to allow the cells in the channel to attach. The Tygon tubing is then unclamped and used for media delivery as shown in Figure2.1c. However, in each case, delivering media by the system configured as shown in Figure 2.1c, all cells died during 8 hours of media perfusion.

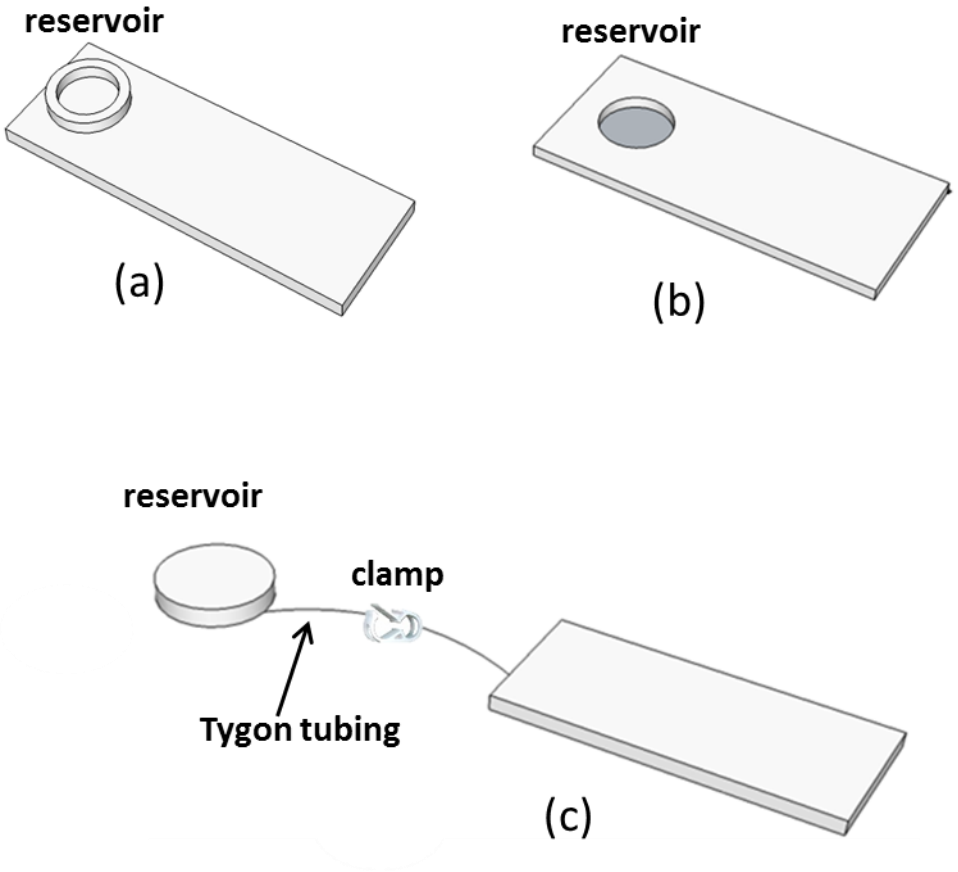

Figure 2.1 Diagram of three different cell growth media delivery systems. (a): on-top design, reservoir was made of PDMS cylinder which set on top of the channel inlet; (b): on-chip design, a hole was cut into the PDMS for use as a media reservoir; (c): off-chip design, media was stored in the Petri dish and delivered through a short length of Tygon tubing. The clamp was closed for 4 hours for cells in the chip to attach, while the remaining cells used for seeding are trapped in the Tygon tubing.

Several possibilities may explain the result. The first is that the flow rate is not suitable for the cells growing in the micro channels. Culturing cells under flow, rather than in static culture dish brings in the concept of shear stress. That some cells are exposed to shear stress *in vivo* due to blood flow could be important to the tissue development. For example, during embryonic development, the embryonic stem cells (ES) are exposed to shear flow from the tissue fluid or blood caused by the beating heart[8]. Studies have shown that fluid stress could induce Flk-1-positive embryonic stem cells differentiation into vascular

endothelial cells *in vitro*[8]. However, under microfluidic dynamic cell culture, the choice of flow rate is not straightforward. On the one hand, microfluidic devices have significantly higher cell surface area to volume ratios than those traditional culture devices. This means that the nutrients in media would be depleted rapidly and the waste products would accumulate[7]. The solution to this problem is to increase flow rate. On the other hand, a fast flow rate could increase the shear stress to a higher level than cells could tolerate. The shear stress in a microfluidic channel could be estimated by equation 2.1 [2]:

$$\tau = \frac{6q\mu}{\omega h^2} \qquad 2.1$$

In which τ is the shear stress, q is the volumetric flow rate, μ is the viscosity of cell culture media, ω is the channel width, h is the channel height. Given the viscosity is $7.987 \times 10^{-4} Pa \cdot s$ (adapted from ref. 2), the channel width is 400 μm, the channel height is 50 μm, with a flow rate of 1 μL/min gives a shear stress of $\tau = 0.7987\ dyne/cm^2$. According to previous studies most cells are viable up to a shear stress of 1 dyne/cm^2 [4, 5]. The flow rate used in microfluidic cell culture should be above the threshold that the cells get enough nutrients and below the threshold that the cells can tolerate the shear stress (Figure 2.2).

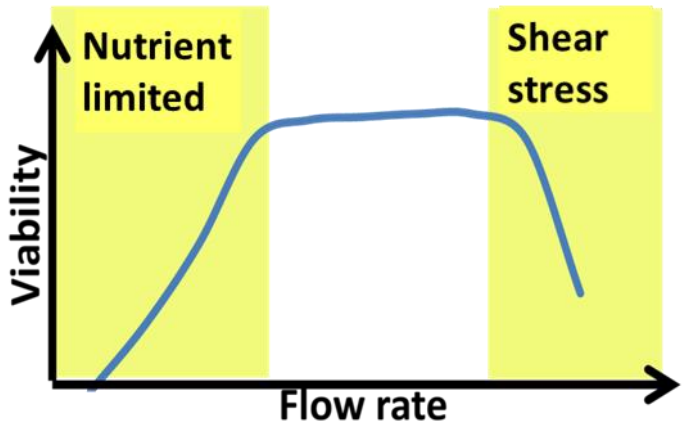

Figure 2.2 The effect of flow rate on cell culture within a microfluidic system (derived from Ref.5)

Different flow rates were evaluated ranging from 0.03 μl/min to 1 μL/min in the off-chip design (Figure 2.1c). But with each flow rate, the cells still die during 8 hours of perfusion. However, cells could be successfully cultured using the configuration shown in Figure 2.1a and Figure2.1b. The biggest difference between the designs shown in Figure 2.1a and Figure 2.1b and that of Figure 2.1c is the elimination of the need for Tygon tubing to deliver cell culture media. As the calculation shows, shear stress is not likely a problem for the flow-rate we use. Alternatively, if shear is not a problem, another hypothesis is that the tubing used to deliver the media is toxic to the cells. Tygon tubing is commonly used in microfluidic cell culture system and is considered biocompatible. However, the Tygon tubing has a low permeability to oxygen, so it is possible that in the 4~6 hours static period when downstream cells attach to the substrate within the device, cells trapped in the tubing can die from anoxia and release toxic components into the surrounding media. This media containing potentially toxic components from dead cells, will be referred as "dead cell conditioned media".

Experiments described below confirm the negative effect of the "dead cell conditioned media" on cells downstream in the microfluidic channel. A possible cytotoxic component of the dead cell conditioned media is lactic acid. Mammalian cells produce large amount of lactic acid during anaerobic respiration. Moreover, cancer cells are unique that under aerobic or anaerobic conditions, cancer cells predominantly produce energy by a high rate of glycolysis resulting in production of high levels of lactic acid in the cytosol[10]. A hypothesis is that during the 4 hours' static period that is used to allow cells to attach to the substrate, the cells in the Tygon tubing produce a high level of lactic acid. Once perfusion is restarted, this high level of lactic acid is toxic to the cells in channel. Studies on cell micro-culture have shown that lactic acid accumulates quickly in a micro well to a level of 10 mM after a 48 hours culture[7]. Thus, it is likely that the lactic acid concentration is high in the tubing where media volume is very small. Studies on the effect of lactate on malignant cells shows that a level of 20 mM lactate increases cell invasion in a Transwell chamber assay[3]. Yet no negative effect of lactate on cell growth has been published.

2.2 Materials and Methods

Device fabrication

The PDMS microfluidic devices used in these experiments consisted of a single 50 μm high, 400 μm wide rectangular channel. The device was fabricated by standard soft-lithography techniques with an SU8 photoresist silicon master. The PDMS microfluidic device was sterilized by a 24 hours soak in 70% ethanol followed by a 24 hours soak in DI water, to remove the uncured PDMS oligomers. After oven drying, the PDMS device was plasma bonded to a clean glass slide. More details about the fabrication process can be found in Chapter 3.

Three designs were tested to deliver growth media to cells growing in the microchannel. One connected the PDMS channel to a 30mm Petri dish as media reservoir with Tygon tubing (off-chip design, Figure 2.3c). Another design used a media reservoir fabricated by cutting a hole with a cylindrical punch at one end of the channel on PDMS (on-chip design, Figure 2.3b). This reservoir held about 300 μL volume. The last was bonding a hollow PDMS cylinder on top of the channel inlet as media reservoir, which held about 1 ml volume (on-top design, Figure 2.3a).

Cell seeding and cell culture

MDA-MB-231 human breast cancer cells were used to test the effect of dead cell conditioned media and lactic acid containing media on cell growth. Cells were cultured in T75 flasks in DMEM + 10% FBS cell culture media until they had grown to 70% confluency before use. Cells were harvested by trypsin from the T75 flask, counted and seeding media was prepared with a density of approximately 1 million cells per milliliter. The glass substrate of all the devices used was incubated with serum containing growth media for 24 hours prior to cell seeding to enhance the cell attachment. For the off-chip device (Figure 2.3c), cells were seeded by gravity through the Tygon tubing from the outlet (syringe pump side, downstream, Figure 2.3c) to the inlet (reservoir side, upstream, Figure 2.3c). When cells came out of the upstream Tygon tubing into the Petri dish reservoir, the Tygon tubing was clamped at both upstream and downstream section to stop the flow and allow the cells in the microchannel to attach. Fresh cell culture media was replenished to the Petri dish reservoir. For the on-chip and on-top design (Figure 2.3b, Figure 2.3a), seeding media was added into reservoir. Cells flowed from reservoir to the outlet Tygon tubing by gravity. The downstream

Tygon tubing was clamped to stop seeding and let the cells attach. Fresh cell culture media was replenished to the reservoir after the remaining cells in it were washed off.

For all the designs the clamp remained closed for 4 hours to let the cells attach in a 37℃ incubator after cell loading. After 4 hours, the clamp was open, the downstream tubing was connected to a media filled syringe via a tubing connecter made form a syringe tip, and the media was drawn from the reservoir by a withdrawing syringe pump at a speed of 0.05 μL/min. All devices were placed in a large Petri dish covered, and kept in a 37℃ incubator. PBS was poured into the Petri dish to prevent evaporation. For the on chip and on-top devices, the media in reservoir was replenished twice a day. Cell numbers were counted twice a day by microscopic examination of the microchannels.

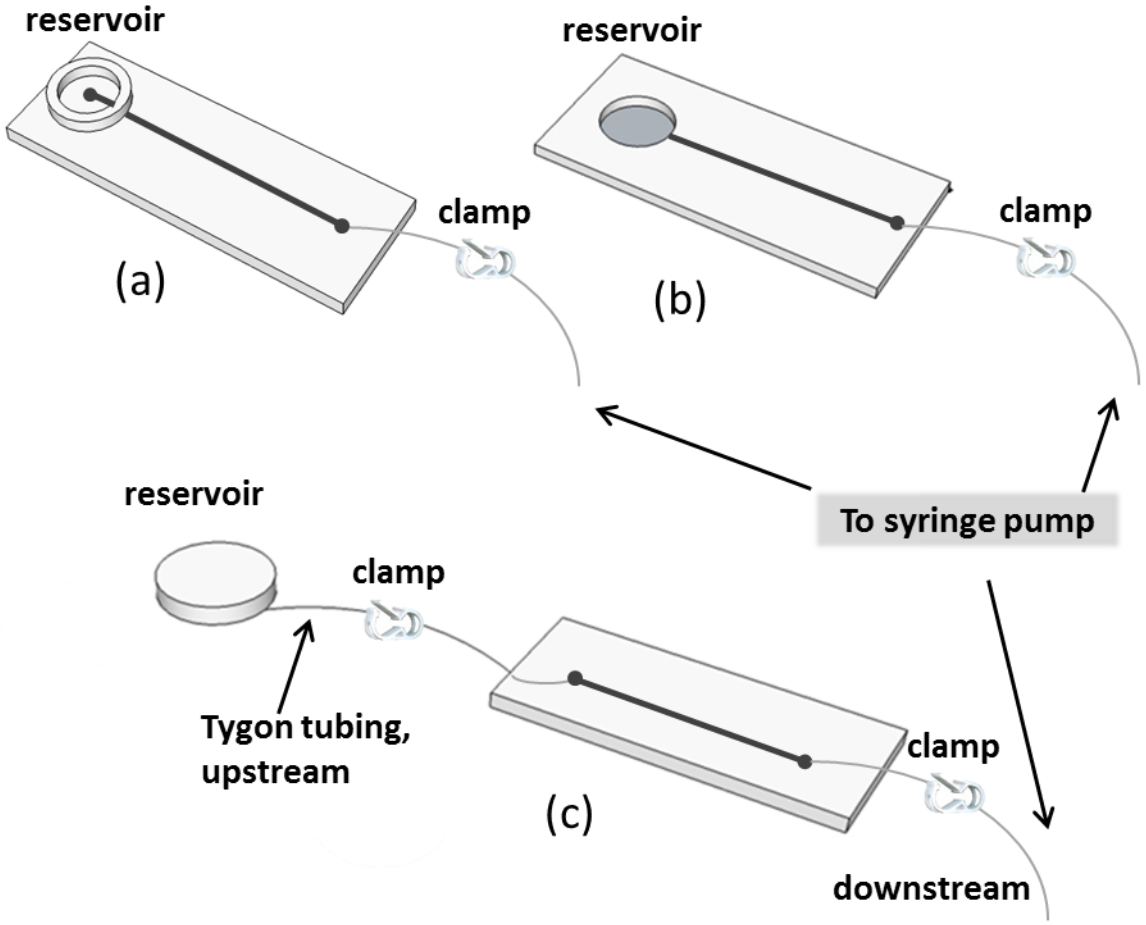

Figure 2.3 Diagram of three different microfluidic cell culture systems; (a) on-top design, media was stored in the reservoir made from PDMS cylinder bonded on top of the channel inlet. Cells were introduced from the reservoir to outlet tubing during the cell seeding process, and the clamp was closed for 4 hours to allow cells to attach. (b) on-chip design, media was stored in the reservoir made by cutting a hole in the PDMS chip. The cell seeding process is similar to that of the on-top design. (c) off-chip design, media was stored in the reservoir made from the Petri dish. Cells were introduced from downstream Tygon tubing to the upstream Tygon tubing. Both clamps were closed during the cell attachment process.

Dead cell conditioned media and Lactic acid/lactate media

A large volume of dead cell conditioned media was prepared by filling a long length of Tygon tubing with cell seeding media (approximately 2 ml). The Tygon tubing was clamped at both ends and put into incubator for 6 hours. After 6 hours the media was collected into a 15 ml conical tube by pushing air into one end of the tubing with a syringe. The media was diluted with fresh cell culture media at a ratio of 1:1 to

exclude the effect of nutrient depletion. The diluted media was centrifuged for 5 minutes to remove any remaining live cells, dead cells and cell debris. A small volume of uncentrifuged media was mixed with 3 ml cell culture media in a 30 mm Petri dish, which was put in the incubator to test the viability of any collected cells. As a control, normal culture media was diluted with PBS at a ratio of 1:1 to compare with the diluted dead cell media.

To explore the possible cytotoxic factors in dead cell conditioned media, 20 mM lactic acid in normal cell culture media were used to study its effect on cell growth. To test whether the effect of lactic acid on cell growth came from lactate or its acidity, sodium hydroxide solution was used to adjust the pH of 20 mM lactic acid culture media to 7.8, whereas the unadjusted 20 mM lactic acid has a pH of 6.59. The adjusted lactic acid media was also used in comparison with original 20 mM lactic acid culture media. Lactic acid media was made by dissolving L-lactic acid (Sigma^{TM}) powder in normal cell growth media. The media was sterilized by a syringe filter.

MDA-MB-231 cells test for dead cell conditioned media

Three on-top devices were used for each group. Normal media was 1:1 diluted with PBS (PM) as a control. Dead cell conditioned media (DM) was used to see its effect on the growth of MDA-MB-231 cells. Both PM and DM were introduced into the device once the cells were attached and after the perfusion started. Cell numbers were counted once a day.

The effect of acidity

On top designed devices and MDA-MB-231 cells were used to test the effect of acidity. 20 mM lactic acid media (pH=6.95) and pH adjusted lactate media (pH=7.8) was used. Normal media was used as control.

2.3 Results

Cell growth in on-chip on-top and off-chip designed device

The growth of MDA-MB-231 cells in on-top, on-chip and off-chip designed device is studied. Each device design has three replications. The cell number in each device is shown in Figure 2.4. The result shows that most of the cells growing in the off-chip devices die within 10 hours of media perfusion, while cells growing in on-chip and on-top designed device survived the three day culture period.

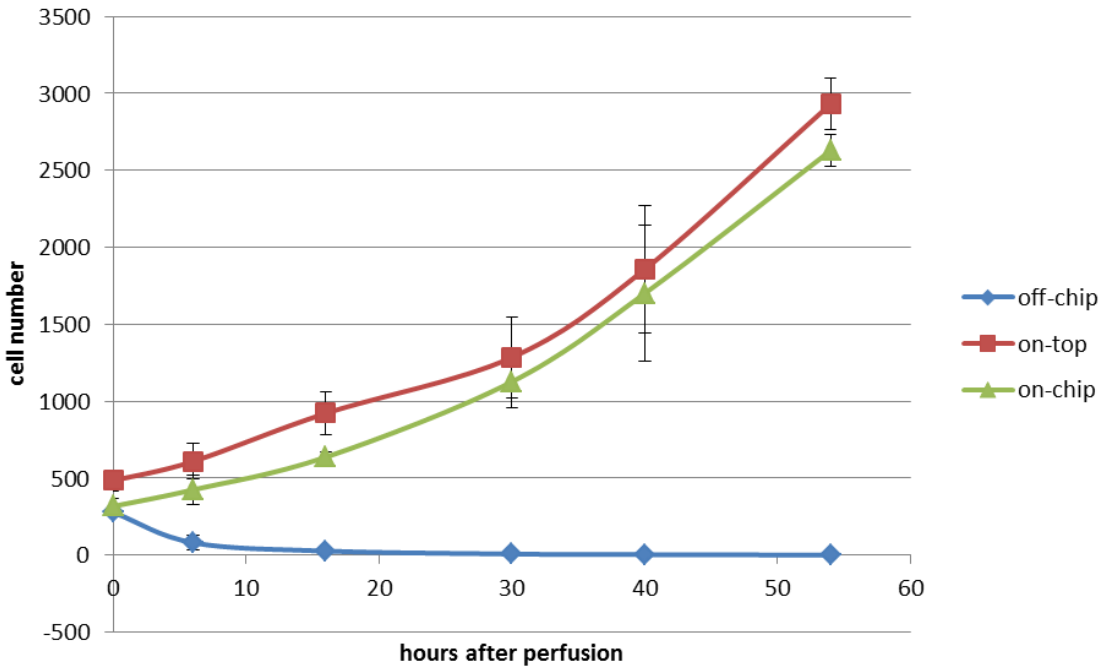

Figure 2.4 MDA-MB-231 cells cultured in off-chip, on-chip and on-top devices. Most of the cells in the off-chip device die within the first 10 hours of media perfusion.

MDA-MB-231 cells test for dead cell conditioned media

PBS diluted media, PM, was used to test whether that if the effect of dead media on cell growth is caused by nutrient depletion. The on-top device with PM shows that MDA-MB-231 cells grow well in this half-diluted media, and the growth rate of cells cultured with PM has no significant difference from the growth rate of those grow in normal media (Figure 2.5, Figure 2.6). However, the cells cultured in DM hardly grow, and begin to die quickly after 40 hours of media perfusion (Figure 2.5). A Student's t-test shows that the growth rate of cells cultured in DM is significantly different form the growth rate of those cultured in NM and PM (Figure 2.6). At the end of this experiment, the pictures of cells cultured in DM and cells cultured in PM were taken with the microscope camera. Most of the cells left in DM are round. Some of them have a huge amount of black dots in cytoplasm. Also, the enlarged nuclei of these cells are characteristic of cells undergoing apoptosis (Figure 2.7).

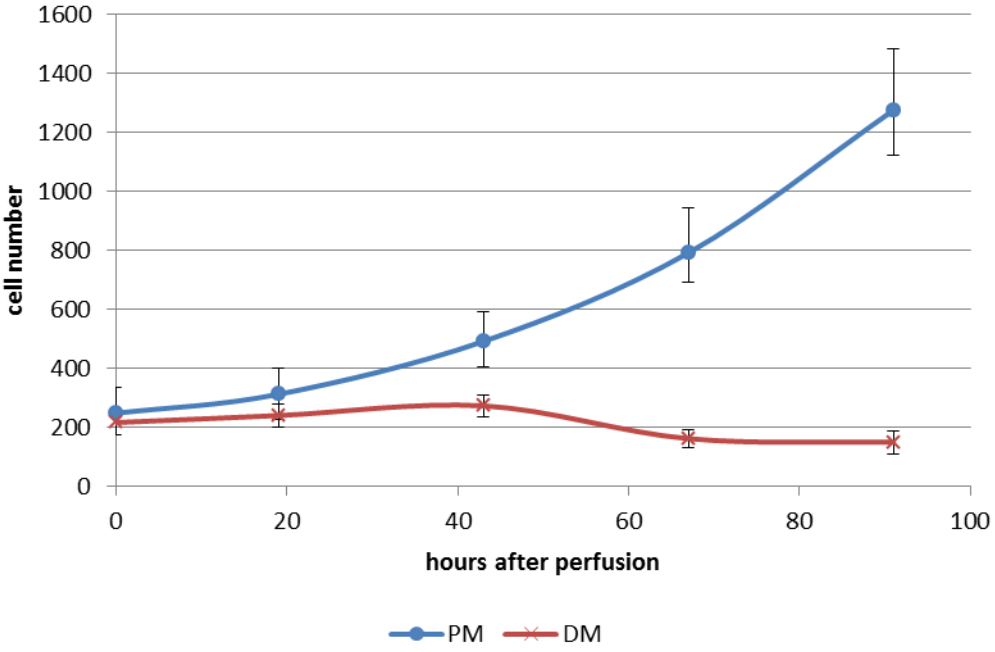

Figure 2.5 MDA-MB-231 cells cultured in PM and DM. The cells cultured with PM grow well in the microchannels, while cells cultured in DM grow very slowly at the first 40 hours media perfusion and start to die after that. PM: PBS diluted media; DM: dead cell conditioned media.

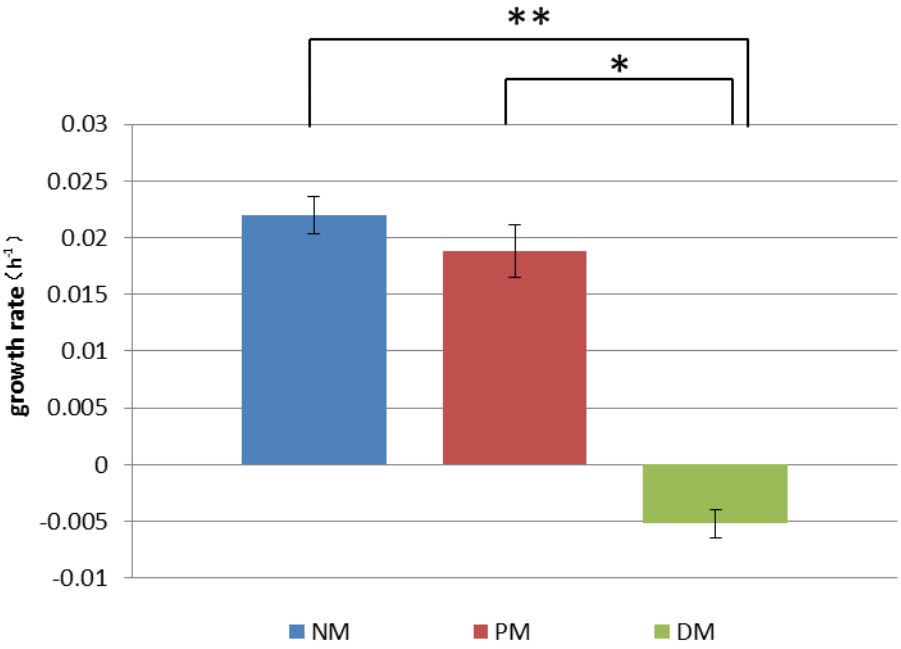

Figure 2.6 The growth rate of MDA-MB-231 cells cultured in NM, PM and DM. There is no significant difference between NM and PM cultured cells. The growth of cells cultured in DM is significantly slower than those cultured in NM and PM. NM: normal media; PM: PBS diluted media; DM: dead cell conditioned media.*:$p<0.05$; **$p<0.01$

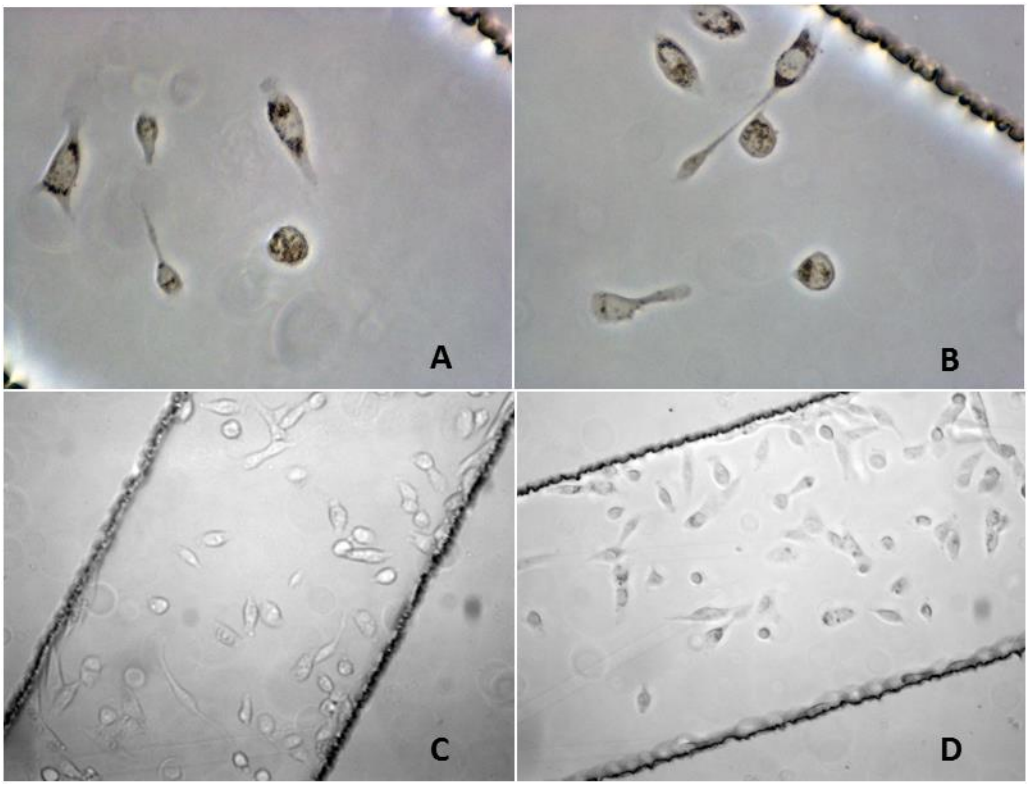

Figure 2.7 MDA-MB-231 cells cultured in PM (C,D) and DM (A,B) The cells cultured in DM are either round or with a morphology similar to cells undergoing apoptosis. The nuclei of cells cultured in DM are enlarged, and there are black dots accumulated in the cytoplasm (A,B).Pictures were taken at the fourth day of media perfusion.

The effect of lactic acid on the growth of MDA-MB-231 cells

The effect of 20 mM lactic acid on MDA-MB-231 cells growth was tested with on-top designed device (Figure 2.8, Figure 2.9). Four devices of normal media and six devices of lactic acid media were used. An unpaired t-test shows that the growth rate of cells cultured in lactic acid media is significant less than the growth rate of cells cultured in normal media were statistically different ($p = 6.19 \times 10^{-6}$). An ANOVA test also shows the growth rate of cells growing in lactic acid media and cells growing in normal media is different ($p = 7.37 \times 10^{-6}$). The growth rate was derived by linear fitting the slope of cell growth curve in

Excel. The cell growth curve was derived by the natural logarithm of cell number over time (Figure 2.8). Cells were counted and fed once a day. It can also be observed that the cells grown in lactic acid media grow slower after 60 hours perfusion, especially in the rear section of the channel (Figure 2.8). It is possible that the cells in the channel produce waste that further affects their growth.

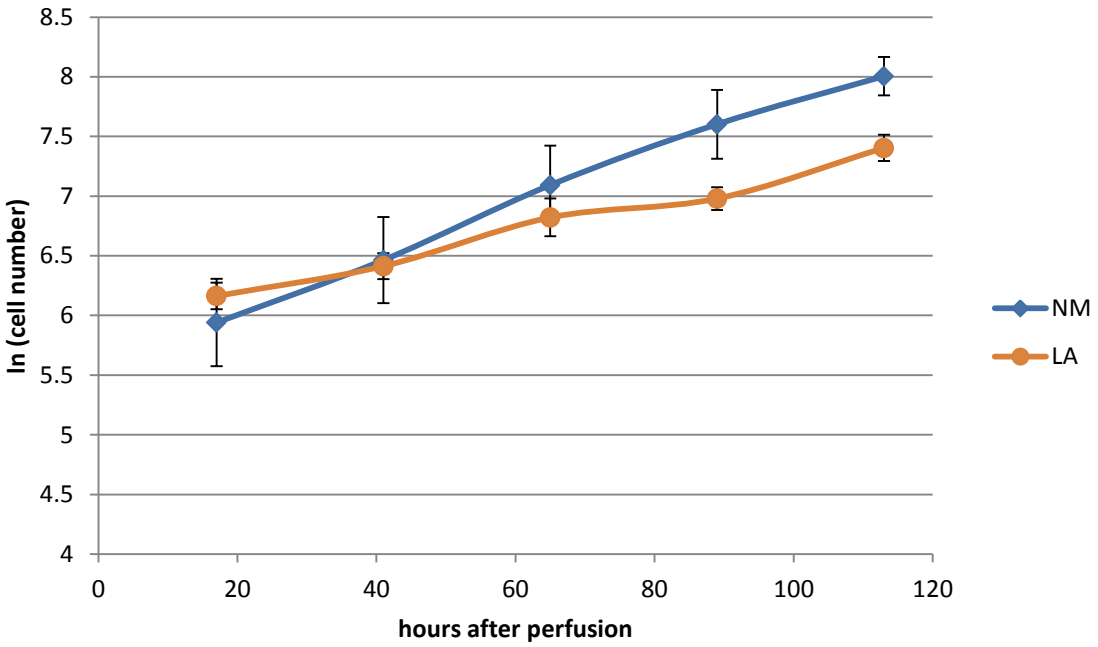

Figure 2.8 Growth rate of MDA-MB-231 cells with normal and lactic acid media. Y axis is derived by the natural logarithm of the cell number.

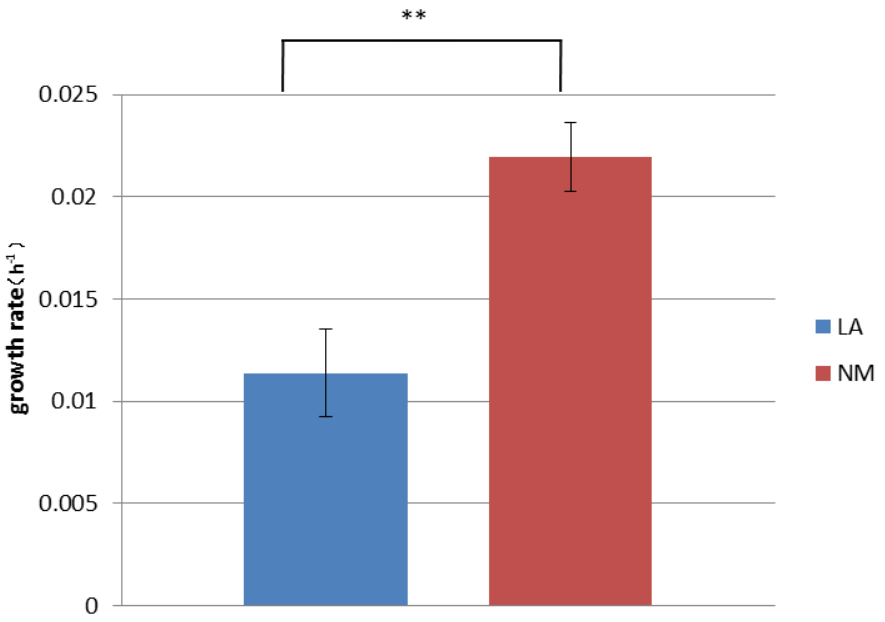

Figure 2.9 Comparison of growth rate of MDA-MB-231 cells in NM and LA. The result shows that MDA-MB-231 cells grow faster in NM. NM: normal media; LA: lactic acid media; $p<0.01$

2.4 Discussion

The negative effect of dead media on cell growth suggests that in micro-scale cell culture, the method used to deliver media is important, especially in the design where the media is delivered from an off-chip reservoir to the cell culture device through Tygon tubing. Since switching tubing could introduce air bubbles which are destructive to cells in the channel, most of the procedures should avoid disconnecting and reconnecting tubing into the device after the channels are filled with media. Air bubbles in microchannels are fatal to cells because the liquid-air interface could rupture cells when they flow through the channel. However, the cell seeding method we use for the off-chip devices leads to a large amount of cells trapped in the Tygon tubing used for media delivery (i.e. the upstream Tygon tubing shown in Figure 2.3c). Our results show that these cells trapped in the media delivery tubing cause a negative effect on the viability of the cells in the microchannel. Another explanation, such as the formation of air bubbles in the

media delivery Tygon tubing when the temperature changes from room temperature to the temperature in the incubator, could also explain the cell death in the microchannel of off-chip designed device after perfusion started. However, these air bubbles are seldom observed in the off-chip devices. Due to the difficulty in accurately controlling the amount of cells that are seeding into the device by gravity, it is hard to eliminate the cells trapped in the media delivery Tygon tubing in these off-chip devices. As a result, on-chip and on-top devices are preferred, because these two designs link the media reservoir directly to the cell culture microchannel. MDA-MB-231 cells could be successfully cultured in on-top designed and on-chip designed devices.

"Dead cell conditioned media" is made with Tygon tubing to prove the hypothesis mentioned above. The results show that dead cell conditioned media also has a negative effect on the viability if cells on-top and on-chip devices when this media is placed in these reservoirs. The reason that the dead cell conditioned media is fatal to downstream cells is not fully explored. There is the likelihood that cells may release some pro-apoptosis signal and/or digestive enzymes during apoptosis/necrosis. It is also likely that cells produce a huge amount of aerobic metabolic waste before dying from oxygen depletion, increasing the media acidity and producing an adverse environment for downstream cells. Interestingly, it is believed that aerobic respiration waste seems to have a positive effect on cancer cells. Previous studies have shown that lactate could increase epithelial cancer cell migration and promote a cancer stem cell phenotype[(1)], which indicates poor clinical outcomes[(1,3)]. Though lactate has not been found to promote tumor growth, 3-hydroxy-butyrate (a ketone body) which is also an end product of aerobic glycolysis, significantly promotes tumor growth *in vivo* due to the "reverse Warburg effect"[(1,3,6)]. Our studies show that lactate/lactic acid has a negative effect

on tumor growth, but not as severe as dead cell conditioned media. However, it is not necessarily contradictory to previous results suggesting aerobic metabolism waste boosts tumor growth[3], since different culture methods are used and different molecules are tested. The effect of lactic acid's acidity is hard to test, because lactic acid induced pH changes in the media will be buffered by the carbon dioxide in the incubator. In 15 minutes the color of lactic acid media turns from yellow to light pink, indicating a rise in pH. As a result, it is hard to test the effect of acidity of lactic acid in our PDMS microfluidic device under carbon dioxide atmospheres. The comparison of growth rate between cells grown in lactic acid media and pH adjusted lactic acid media shows no significant difference. In conclusion, cell death observed in off-chip designed device has been confirmed. What needs to be further studied is the substance in the dead cell conditioned media that causes cell death in the microchannels.

Chapter 3. A Tumor-on-a-Chip for Studying Oxygen Gradient Induced Breast Cancer Cell Metastasis

The first chapter discussed the role of hypoxia in cancer metastasis. Cancer cells cultured in a low oxygen atmosphere which models hypoxic regions of tumors often show increased metastatic potential. In this chapter, the design of a tumor-on-a-chip PDMS device is described. In this design, a gas channel layer sits directly above a cell channel layer. The gas channel layer enables the control of oxygen level and the creation of spatial heterogeneity of oxygen concentration in the media of the cell channel layer. The cell channel layer functions as an invasion assay with cells trespassing Matrigel blocked, capillary sized invasion channels. The oxygen gradient created by our device is experienced by a metastasizing cancer cell as it migrates from the hypoxic tumor channel into the oxygen-rich vasculature channel. With an on top reservoir sits on the device, the media is withdrawn through the cell culture channel, and is replenished each day. Ideally, the cells can be cultured for as long as necessary. MCF7-0 and MDA-MB-231 cancer cells have been cultured in the device in order to determine the effect of oxygen content and an oxygen gradient on cell metastasis.

3.1 Introduction

As introduced in Chapter 1, solid tumors often contain regions of hypoxia with pO_2 less than 10 mmHg[7,20]. Moreover, the chaotic blood vessel structure in tumors creates a fluctuation of oxygen level between moderate hypoxia to nearly anoxia, with cycling periods from minutes to days[2,13]. More and more studies have suggested that hypoxia and hypoxia/re-oxygenation are related to aggressive behavior and therapy resistance, and promote a cancer stem like phenotype[8,11,17,19]. Since the study of hypoxia is important to

fully understand the cancer metastasic process, extensive research has been done concerning the effect of hypoxia on cancer cell aggressiveness. Many of these *in vitro* studies involve the use of Boyden chambers or Transwell® chambers placed in a hypoxic or normoxic conditions[6,9,18], and *in vivo* studies involve tumor clamping, transit embolization or directly putting tumor-bearing mice in hypoxia/re-oxygenation cycles[3,15,22]. However, for different reasons, these studies cannot accurately control the oxygen level experienced by the tumor cells. It takes hours for the oxygen level in the media of Boyden chambers to equilibrate to that of the atmosphere. This means that such a method is not able to reproduce the periodic changes characteristic of cycling hypoxia, which has cycles ranging from minutes to hours to days[7]. Boyden and Transwell chambers also are unable to model the transition from low to high oxygen level experienced when a cell leaves the hypoxia environment tumor environment and intravasates into the oxygen-rich circulatory system (Figure 3.1). The oxygen-rich circulatory system has been shown to be cytotoxic to 'weakly metastatic' cells[10].

To better mimic the oxygen level experienced by cancer cells in a solid tumor, a double layer PDMS microfluidic device was designed (Figure 3.2 C, D). The tumor-on-a-chip is based on a previously published design which studied cancer cell metastasis thorough blood capillaries[4,5]. The tumor-on-a-chip device adapted this design with capillary-sized, Matrigel-blocked perpendicular migration channels joining two cell channels. The cell channels and the migration channels on the bottom cell channel layer function as an invasion assay allowing cancer cells to migrate through an extracellular matrix. The Matrigel blocked, 10 micron sized migration channels resemble the Matrigel coated porous insert of a

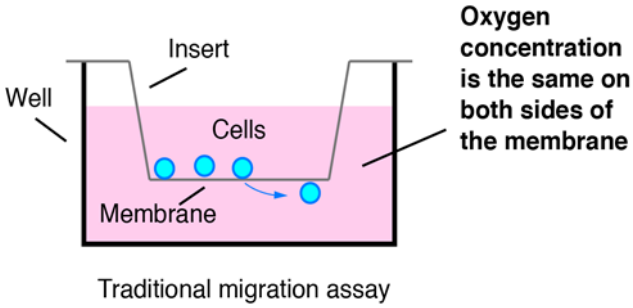

Figure 3.1 Invasion/migration assays in a classic Transwell chamber are performed under non-varying pO_2.

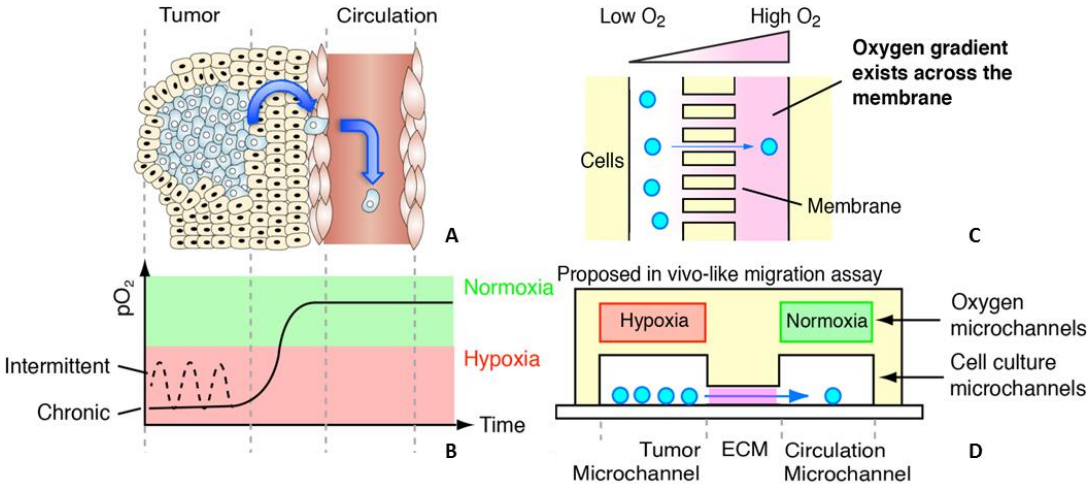

Figure 3.2 Overview of the Tumor-on-a-chip. A: A cancer cell experiences three regions of changing pO2 upon migrating from the tumor and penetrating the circulatory system. B: A sketch of the time dependence of the change in pO2 across these regions. C: A top view of the device showing migration of cells from low to high oxygen regions. D: A cross section of the tumor-on-a-chip that can mimic these changes in pO2 across these regions.

Transwell chamber[24] (Figure 3.1, Figure 3.2C). However, our device has the advantages over the Transwell chamber in that the number of all the cells in the channel could be accurately counted, whereas the Transwell chamber are difficult to qualify[25,26,27]. For example, only individual fields could be counted in a

single Transwell chamber. This could lead to erroneous result, if the cells are not spread uniformly[26]. Moreover, the cells which have traversed the pores and then detached the filter of the Transwell chamber are often neglected[26]. Finally, an oxygen gradient cannot be achieved with a Transwell chamber assay. The high gas permeability of PDMS and the micron scale distance between cells and gas sources achieved by multilayer lithography techniques enables rapid gas diffusion, thus creating and maintaining the desired oxygen landscape across the cell culture channels[1,12,14,16]. This difference in pO_2 resembles that experienced by metastatic cancer cell when it migrates from the hypoxic tumor into the oxygen-rich vasculature (Figure 3.2). With these two characteristics put together, the tumor-on-a-chip device provides us an innovative, promising method to delineate the mechanism of cancer metastasis under hypoxia, boosting the emerging research of tissue-on-a-chip[23]. Both of the effect of chronic hypoxia and intermittent hypoxia could be studied with this tumor-on-a-chip device. The metastatic cells which invade through the migration channels could be collected. Then the cell's response to hypoxia and oxidative stress, for example the expression of HIF-1α, osteopontin, VEGF and MMP1 markers could be analyzed.

3.2 Materials and Methods

Device fabrication

The tumor-on-a-chip device was fabricated with standard soft-lithography techniques. The master for each channel was fabricated by spin coating SU8 photoresist on to a silicon wafer. The air channel master required only a single coating and a single UV exposure, while the cell and migration channels demanded a second coating on top of the first developed migration channel layer (Figure 3.3, Figure 3.4).

In fabrication of the cell channel master, the migration channel patterns were fabricated first. The first step was to spin coat SU8 3010 on to a clean silicon wafer at a speed of 3000 rpm for 30 seconds with a spin coater. This yielded a 10 microns layer of SU8 on the silicon wafer (Figure 3.3A). After the spin coating, the wafer needed to be pre-expose baked. The wafer was first baked at 65℃ for 5 minutes on a hotplate to flatten the SU8 and then transferred to 95℃ hotplate to bake for another 15 minutes to volatilize the solvent in the SU8. All the baking should be conducted in a vent hood and with a cover on the hotplate. The following step was UV exposure, where the SU8 was exposed to UV light, crosslinking and forming the patterns we need to fabricate the PDMS device (Figure 3.3B). The pre-expose baked wafer was then covered by the migration channel mask, which blocked UV light except at the patterns channels. The exposure time was 50 seconds. A UV filter was put on top of the wafer and the mask to filter out unwanted wavelengths. The next step was post-expose bake, where the solvent was further volatilized from the SU8 and the adhesion between patterns and wafers was strengthened. The post-expose bake required 2 minutes at 65℃ and 15 minutes at 95℃. The wafer was left on the hotplate which had been turned off after post-expose baking until fully cooled. Then the wafer was gently submerged into SU8 developer for 5 minutes without swirling the dish to develop (Figure 3.3C). The developer dissolves the uncrosslinked SU8 on the wafer, only the crosslinked patterns were left. The developed master was hard baked by covered baking on a 150 ℃ hotplate for 40 minutes to harden the patterns. The master was then left on the hotplate which had been turned off to gradually cool down to room temperature to prevent heat shock that can separate the patterns and wafer.

The cell channel patterns were built on top of the migration channel patterns. The wafer with migration channels pre-made was again spun coat with a 50 microns layer SU8, by spin coating SU8 2050 at 3000 rpm for 30 seconds with spin coater (Figure 3.3D). This was followed by pre-expose bake at 65℃ for 3 minutes followed by 95℃ for 10 minutes. Then, a cell channel mask was put on top of the wafer and aligned with the migration channel patterns. The alignment was done by firstly taping the wafer on top of a hard paper board. The cell channel mask was then taped on to the same paper board on top of the wafer, with the alignment squares of the mask and of the patterns on the wafer co-registered (Figure 3.4). The alignment was checked by microscopic examination. If the alignment was unacceptable, the alignment step was repeated, until the migration channels patterns were aligned with the cell channels patterns on the mask. After alignment, the SU8 on the master was exposed with UV light for 35 seconds, with UV filter on top (Figure 3.3E). The development step is followed by the post-expose bake step, at 65℃ for 3 minutes and 95℃ for 10 minutes. The post-expose baked and then cooled master was submerged in SU8 developer for 7 minutes, the developer dish is gently swirled during the development to help dissolve the uncrosslinked SU8 (Figure 3.3F). The last step is the hard bake, at 150℃ for 40 minutes. After fabrication, the cell channel master was silanized by Trichloro(ctyl)silane to facilitate the release of PDMS in the following steps.

The gas channel master was fabricated with similar process, except it only required a single spin coating and a single UV exposure. Briefly, a layer of 100 microns SU8 was spun coat on top of a clean master wafer with spin coating SU8 2050 at 1720rpm for 30 seconds in spin coater. The pre-expose bake was at 65℃ for 5 minutes and at 95℃ for 20 minutes. The exposure time was 40 seconds with mask and UV filter on top

of the master. The post-expose bake was at 65℃ for 5 minutes and at 95℃ for 10 minutes. The development was conducted after the master was cooled after baking, by submerging the master in the SU8 developer for 10 minutes with gently swirling of the developer dish. At last, the gas channel master fabrication was finished by hard baking at 150℃ for 40 minutes and then cooling down slowly.

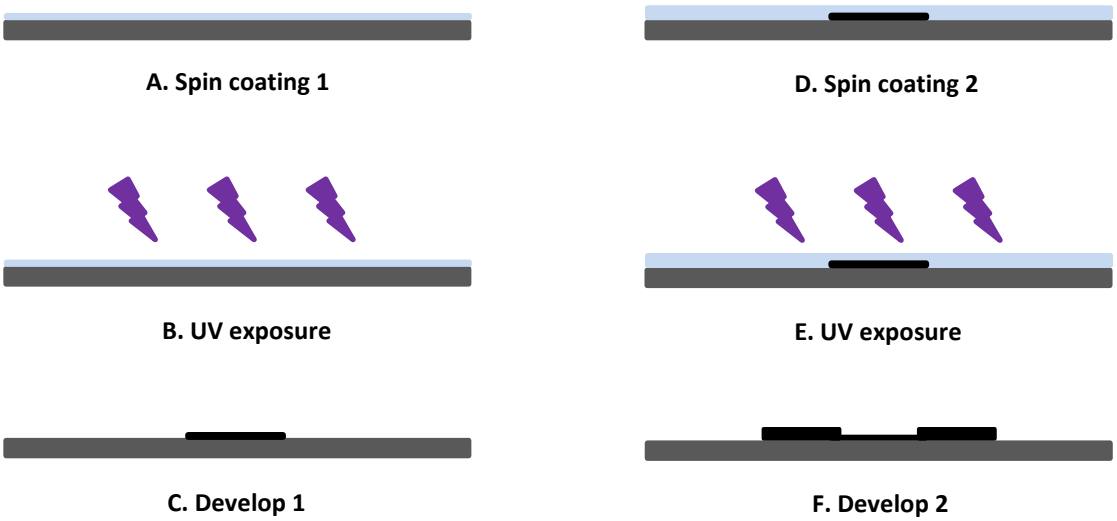

Figure 3.3 Cell channel master fabrication diagram for tumor-on-a-chip; Cell channel pattern was stacked on top of the migration channel pattern, by a second spin coating of SU8 photoresist

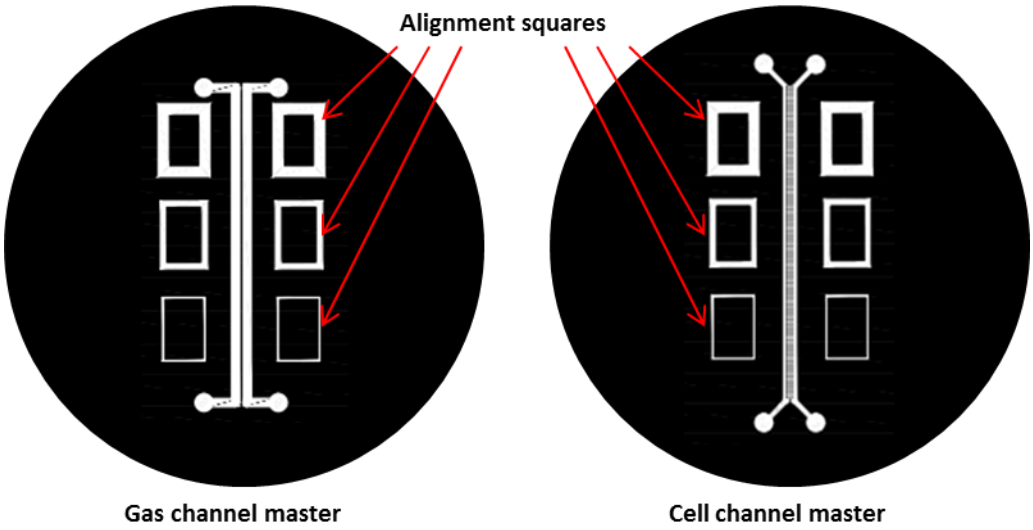

Figure 3.4 Diagram of the gas channel master and cell channel master. The red arrows show the locations of the alignment squares. The alignment squares were used in aligning the cell channel mask and migration channel patterns during cell channel master fabrication, as well as in aligning the gas channel PDMS chip and cell channel PDMS layer.

PDMS silicone elastomer was mixed with curing agent in a 10:1 ratio. The mixing was done with a plastic fork and continued for 5 minutes to ensure a complete mix. After mixing, the uncured, pre-mixed PDMS was put into a desiccator to get rid of the air bubbles trapped in PDMS by vacuum. An gas channel layer was fabricated by pouring 27.5 grams uncured, pre-mixed PDMS on to an aluminum foil disk containing air channel master (Figure 3.4) and then baking on a hotplate at 90℃ for 1 hour. The finished gas channel layer was drilled with six holes at the alignment squares (As the alignment squares in Figure 3.4) to help the gas diffusion in the following binding step. The cell channel layer was made by spin coating uncured, pre-mixed PDMS on to cell channel master at 890 rpm for 1 minute to get a desired thickness of 100 microns. The PDMS was left in room temperature for 10 minutes to flatten out the uncured PDMS, then baked at 90℃ for 1 hour (Figure 3.5A,B).

The bonding of the gas channel layer to the cell channel layer was performed by a “stamping technique”. Uncured PDMS was spun coat on a clean silicon wafer at 3000 rpm for 30 seconds to yield an ultrathin layer of approximately 25 microns (Figure 3.5C). The gas channel layer was stamped on top of this uncured PDMS, and then placed on top of cell channel layer (Figure 3.5D). The uncured, stamped PDMS on the bottom of the gas channel layer serves as a glue to bind the gas channel layer to the cell channel layer (Figure 3.5E). The position of the gas channel layer was corrected by aligning the alignment squares designed on both layers (As in Figure 3.4). After removing the air bubbles trapped between these two layers via vacuum, the two layers were baked at 90℃ for 1 hour to finish bonding (Figure 3.5F). Due to the thinness of the cell channel layer and the glue binding layer, uncured PDMS was poured around the bonded

device, baked at 90 ℃ for 1 hour to help the release of the device from the master. The finished device was soaked in 70% ethanol for 24 hours followed by in DI water for 24 hours to remove the uncured PDMS oligomer. The cleaned device was dried by baking in oven at 80℃ for 2 hours, then bonded to clean glass slide by plasma treatment.

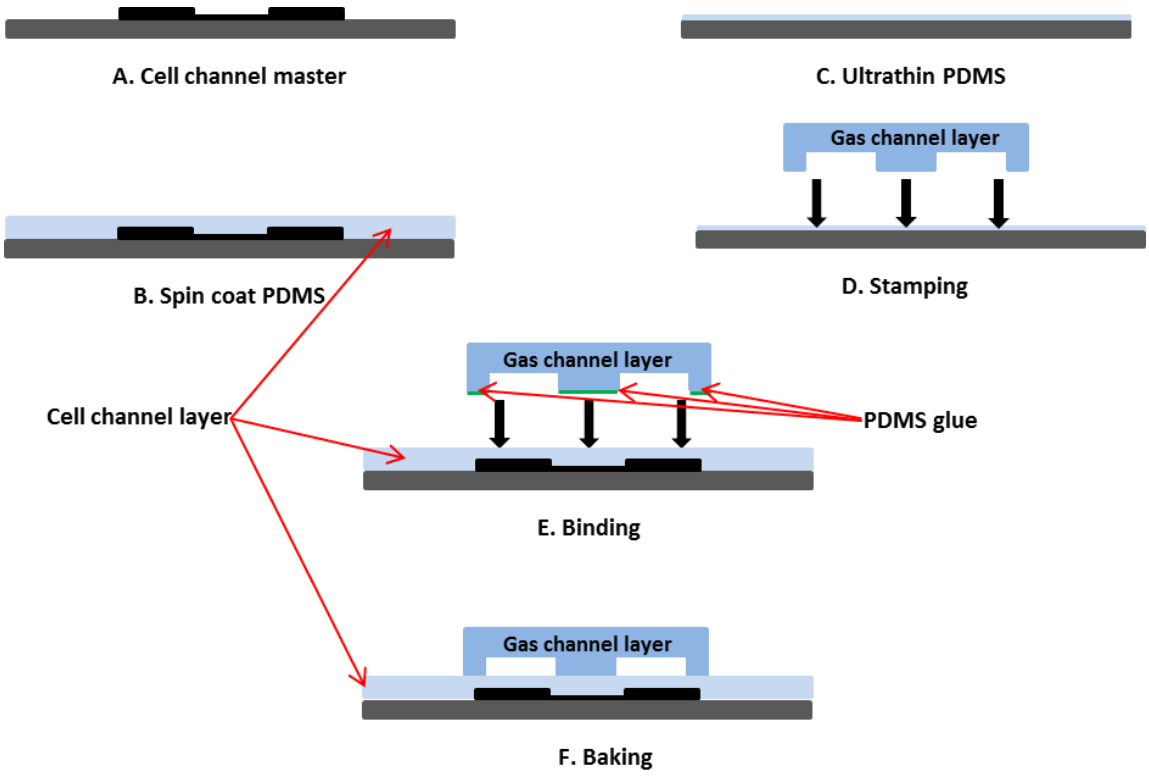

Figure 3.5 Tumor-on-a-chip fabrication diagrams. The gas channel layer was stamped (D,E) on the ultrathin PDMS layer as glue, and then bonded to cured cell channel layer.

Matrigel filling

Matrigel is a gelatinous protein mixture that stays fluid at low temperature and gels at higher temperature. Thawed, cold-Matrigel was double diluted with serum-free DMEM, and kept cold before use. A cold tumor-on-a-chip device was kept on an ice pack. Cold Tygon tubing was connected to the four gas channel outlets and two cell channel outlets at the opposite site of the reservoir (Figure 3.6A). Matrigel was withdrawn to a cold 1 ml syringe. After the plunger was taken off, Matrigel was introduced to the cell channel through the tubing via gravity. The gravity potential difference is created by raising the syringe above the device about six inches (Figure 3.6B). After the Matrigel filled one side of the cell channel and came out of the outlet, the whole device was kept in refrigerator for 20 minutes (or, overnight) until the

capillary effect filled the migration channels. Then cold cell culture media was put into the reservoir, and the tubing used to introduce Matrigel was lowered, so that the flow direction reversed to wash off the Matrigel in cell channel (Figure 3.6 C). The migration channels retain the Matrigel. Finally, the device was warmed to 37℃ in an incubator for 24 hours to crosslink Matrigel in the migration channels and provide a thin protein coating the glass substrate.

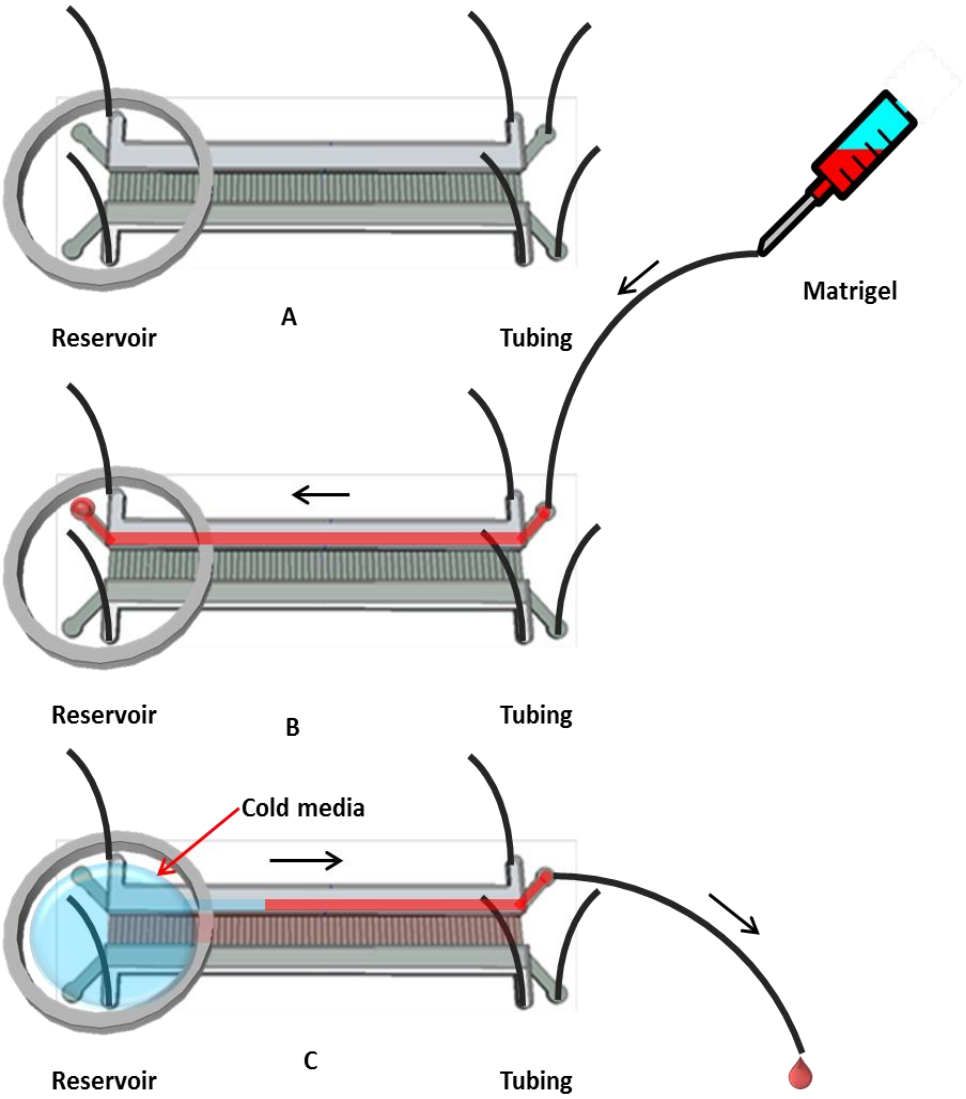

Figure 3.6 Diagram for Matrigel filling in on-top designed tumor-on-a-chip device; A: Tubing were connected to the four air channel outlets and the two cell channel outlets opposite to the reservoir. B: Chilled Matrigel was introduced through the Tubing that has been raised higher than the device. Matrigel fills the main channel and by capillary action is drawn into the migration channels. C: Once the migration channels were filled, cold media was poured into the reservoir while the Tygon tubing is lowered down to change the flow direction. The cold media flowed into the cell channel and washed Matrigel off the cell channel leaving the migration channels filled. The black arrows show the flow direction. The cell channel which was left empty at B and C was named circulatory channel

Media delivery

Three media delivery designs were tested (Figure 3.7). The first was off-chip design, in which media was stored in a 3mm Petri dish and withdrawn to the device through Tygon tubing (Figure 3.7C). The second design was on-chip design, where a hole was punched by a puncher at one of cell channel outlet before the device was bonded to glass. After bonding to glass, the media was stored in this on-chip reservoir and withdrawn through the cell channel (Figure 3.7A). The third one is the on-top design, in which a PDMS cylinder was made with two different sized punchers, stamped on to uncured PDMS as glue and then bonded to the device around the channel outlets at one end. In this design two cell channel outlets and two air channel outlets at one end of the device were included in the reservoir (Figure 3.7B, Figure 3.6A). Media was stored in the on top reservoir and withdrawn through the cell channel. For all the designs media was withdrawn by a syringe pump.

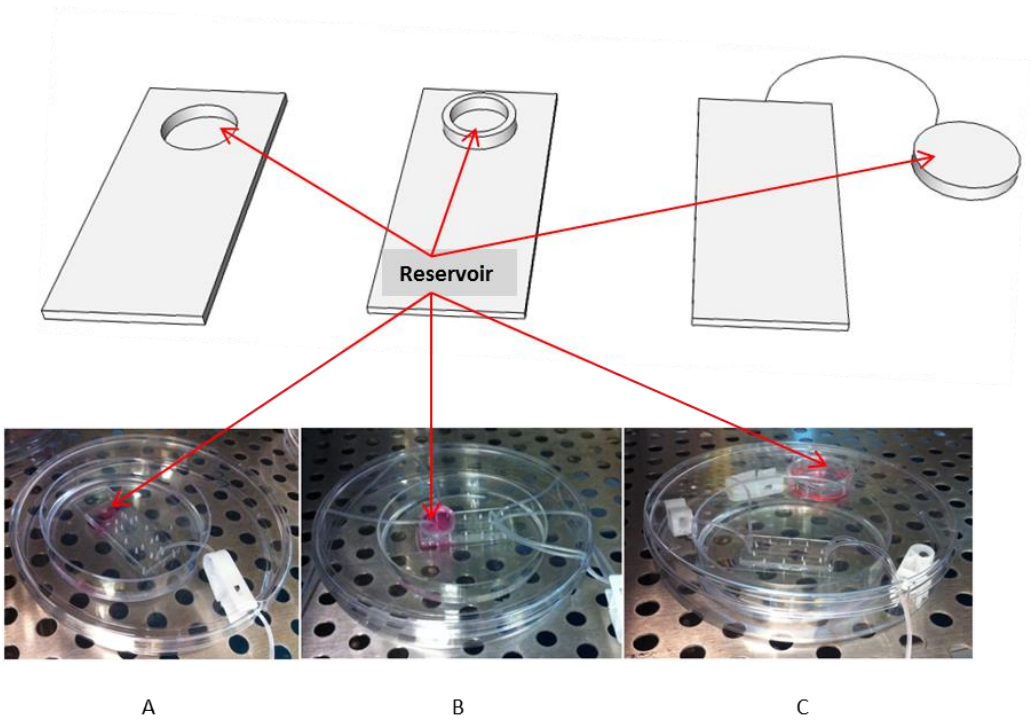

Figure 3.7 The media delivery designs for tumor-on-a-chip device; A: on-chip design, a hole was cutting at one cell channel outlet as media reservoir; B: on-top design, a PDMS cylinder was bonded on top of the device; C: off-chip design, a 30mm Petri dish was used to hold media.

Gas atmosphere control

Hypoxia was set as 1% oxygen[21]. Gas mixtures of 95% air/5% CO_2 (Normoxia gas) or 1% O_2/5% CO_2/94% N_2 (Hypoxia gas) were delivered to the gas channels at a flow rate of 5 mL/min via mass flow controllers (Aalborg, Model GFC17). Gas mixing and flow rates were regulated using these flow controllers under computer control using a custom LabView-based program.

Mathematical Model of Oxygen Distribution

Steady-state oxygen gradients generated within the device were predicted by finite element analysis of oxygen diffusion based on Fick's equations using COMSOL 4.2 software. In our models, the oxygen

diffusion coefficient within PDMS is $2.15 \times 10^{-9}\, m^2/_s$. The atmosphere surrounding the device was set to 20% oxygen. Gas channels contained 20% or 1% oxygen.

Glass cleaning

The glass substrate used for tumor-on-a-chip was first cleaned with ethanol and DI water and dried in an oven at 110℃. The glass was then soaked in Fisherbrand™ chromic-sulfuric acid cleaning solution overnight. The soaked glass was washed with DI water for multiple times and further sonicated in water bath, then baked dry again with same method before use.

Cell seeding and cell culture

MDA-MB-231 and MCF7-0 breast cancer cells were cultured in our tumor-on-a-chip device. Cells were harvested by trypsinization after they had grown to 70% confluency in T75 flask in DMEM + 10% FBS cell culture media. Seeding media was prepared to a density of approximately 1 million cells per millimeter. The glass substrate of all the devices used was incubated with serum containing growth media for 24 hours prior to cell seeding to enhance the cell attachment. For the off-chip device, cells were seeded by gravity through the Tygon tubing from the outlet (syringe pump side, downstream) to inlet (reservoir side, upstream). When cells came out of the upstream Tygon tubing into the Petri dish reservoir, the Tygon tubing was clamped at both upstream and downstream section to stop flow and let the cells in channel settle and attach to the glass surface. Fresh cell culture media was replenished to the Petri dish reservoir. For the on-chip and on-top design, seeding media was added into reservoir. Cells flowed from reservoir to the outlet Tygon tubing by gravity. The downstream Tygon tubing was clamped to stop flow and let the cells settle and attach. Fresh

cell culture media was replenished to the reservoir after removal of the remaining cells. The cell-free channel (i.e. the circulatory channel as the empty channel in Figure 3.7) that was left empty during Matrigel filling was filled with media via gravity after the cells attached.

For all the designs the clamp remained closed for 4 hours to let the cells attach in a 37℃ incubator after cell loading. After 4 hours, the clamp was opened, the downstream tubing was connected to a media filled syringe via a tubing connecter made form a syringe tip, and the media was drawn from media reservoir by a withdrawing syringe pump. Different flow rates ranges from 0.05-0.14 μL/min were tested. The entire device was contained within a Petri dish and was kept in 37℃ incubator. PBS was poured into the Petri dish to prevent evaporation. For the on-chip and on-top devices, the media in the reservoirs were replenished once a day. Cell numbers were counted by microscopic examination once a day.

3.3 Result

Device fabrication

The fabricated tumor-on-a-chip device is shown in Figure 3.8. The two cell channels (400(width) X 50(height) X 30000(length) μm) are connected perpendicularly by parallel migration channels (10 X 10 X 400 μm). 50 μm above the cell channels, are two air channels (800 X 100 X 30000 μm) separated by 300 μm. The two air channels overlay the cell channels and protrude 50 μm into the migration channels, to help the creation of an oxygen gradient.

Matrigel filling

Gravity was used to introduce Matrigel into one of the cell channels. It takes about 2 minutes for Matrigel to flow through the channel and finally comes out of the cell channel outlet and forms a droplet on top of PDMS. However, the migration channels are barely filled at this point. The device then is taken to the refrigerator to let the capillary effect to fill the migration channels while the surface tension will hold the Matrigel at the end of migration channels from entering the other empty cell channels.

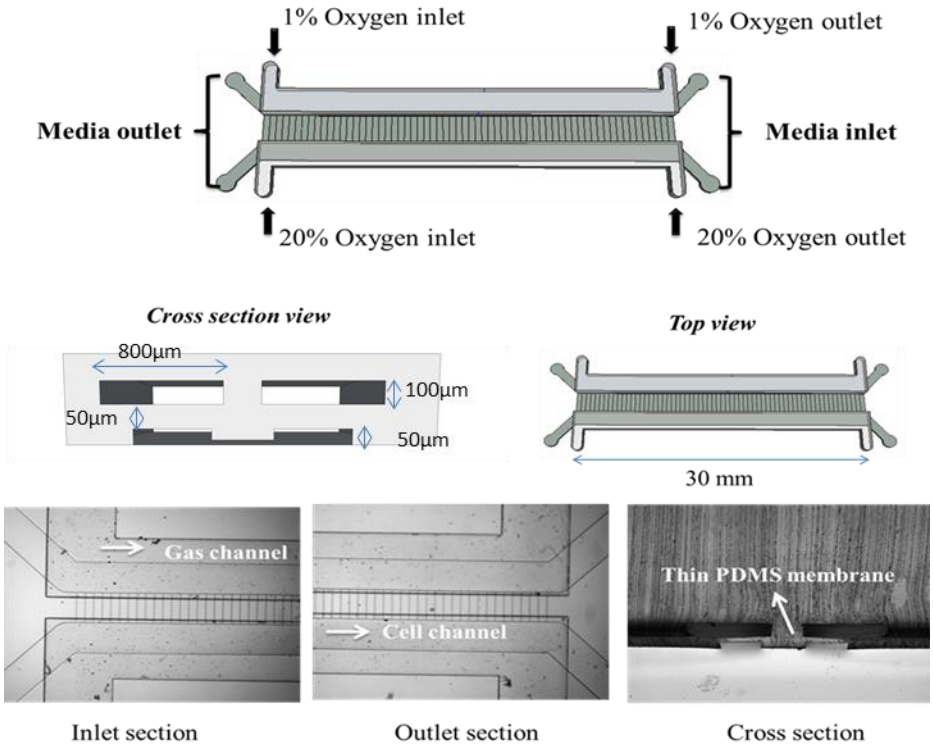

Figure 3.8 The diagram of tumor-on-a-chip. (top) the dimension and position of cell channels and airchannels; (bottom) photos of a fabricated device.

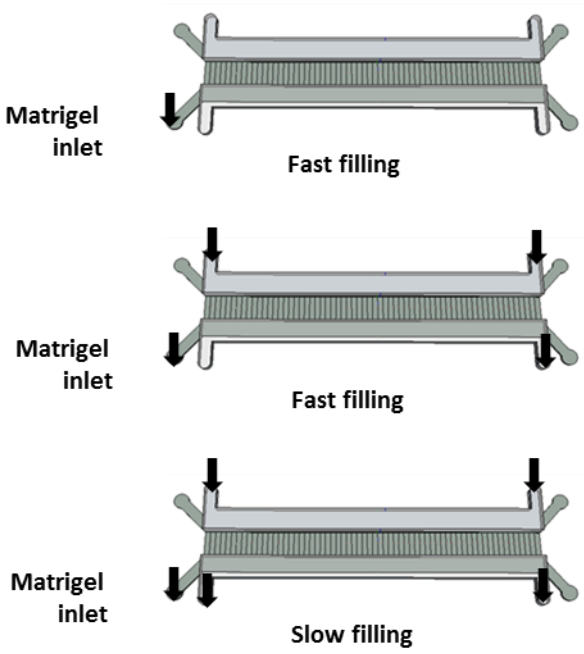

Figure 3.9 Matrigel filling affected by Tygon tubing at the air channel inlet; black arrow shows the position of tubing. The tubing plugged the nearby matrigel inlet slowing the filling of the migration channels.

The time needed to fill the migration channels is roughly 20 minutes, without Tygon tubing plugged into the gas channels. However, the device with Tygon tubing connected to the gas channel requires significantly longer time for the capillary effect to work. The time ranges from 2 hours to some of the devices, to 8 hours. Experiments show that the Tygon tubing plugged into the gas channel outlet near the Matrigel inlet affects the filling efficiency (Figure 3.9). The reason why the tubing in the nearby gas channel would affect migration channel filling is not clear. It could be that the insertion of the Tygon tubing deforms the PDMS near the outlet for the cell channel, thus makes the filling process slower.

Media delivery

As explained in Chapter 2, off-chip design in which cell is trapped in Tygon tubing is problematic is not suitable for cell culture. On-chip and on-top design both work. However, due to the seeding method we use, there are some cells left in the media reservoirs after washing. Untreated PDMS does not support cell attachment but glass does. So in the on-chip design, there are a lot of cells growing in the reservoir's glass bottom and it could deplete the media in the reservoir after 3 days (Figure 3.10), whereas in on top design the PDMS bottom does not support cell growth. In conclusion, the on-chip design is chosen for experiments.

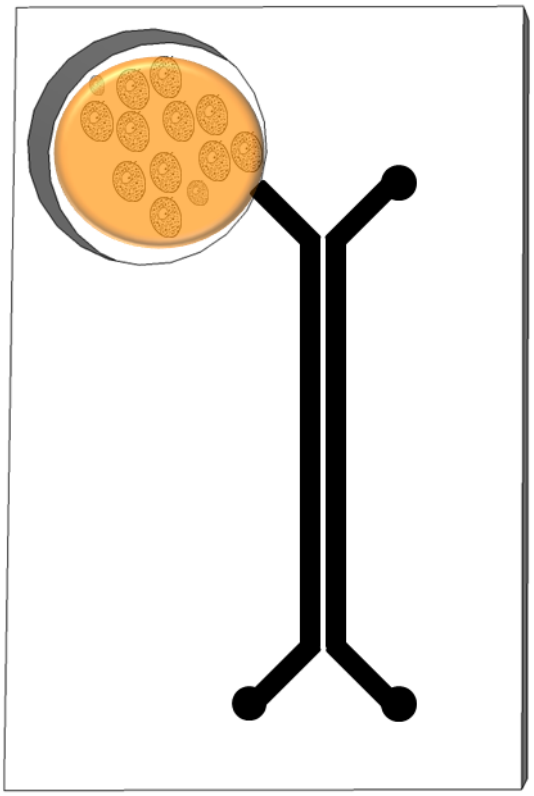

Figure 3.10 Diagram shows that cells growing in the reservoir of on-chip designed device. The media became yellowish when these cells proliferated to a degree that depleted the media.

Mathematical Model of Oxygen Distribution

The diagram for oxygen distribution in the device and the gradient of oxygen thorough the channels is generated by COMSOL (Figure 3.11). The result shows that the oxygen concentration increases gradually from hypoxia cell channel to normoxia cell channel, and the oxygen gradient across the cell channel and migration channels forms an “s” curve. However, it is noticeable that the oxygen distribution is not uniform in the hypoxic cell channel, the oxygen level rises when it comes near to the migration channels (bottom figure of Figure 3.11, the dashed lines depict the position of the two cell channels and the migration channels).

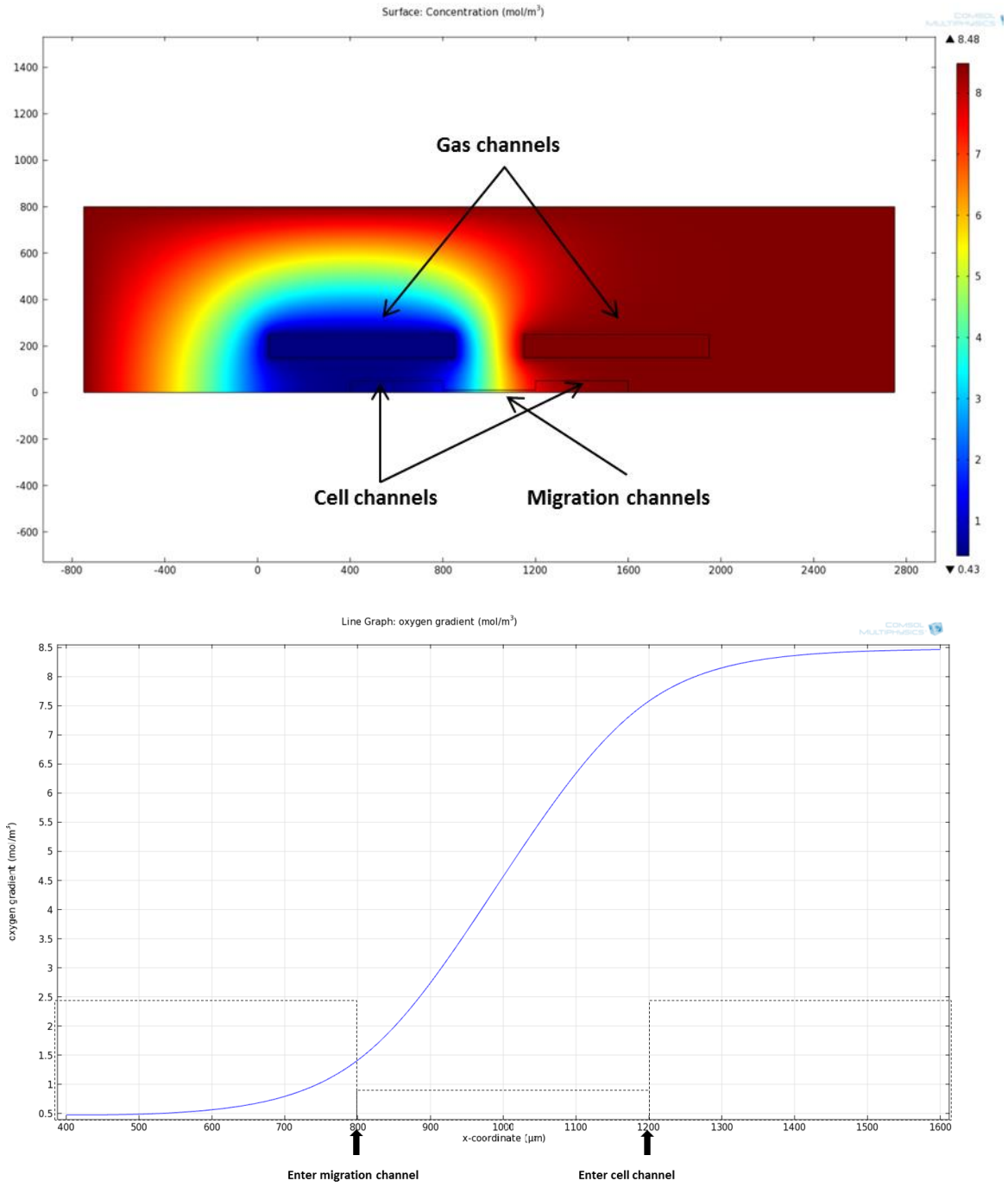

Figure 3.11 COMSOL simulation for the spatial distribution of oxygen landscape across the entire device. The oxygen content ranges from 1% (blue) to 20% (red) (top). For the regions just above the glass surface, where the cells will be located, the oxygen level increases gradually from the hypoxic cell channel to normoxic cell channel, forming an “s” shaped curve.

Cells growth under different flow rates

The flow rates of 0.07 μ L/min and 0.14 μ L/min were used to study the effect of growth media flow on the growth of MCF7-0 and MDA-MB-231 cells (Figure 3.12). A growth rate was derived by determining the slope of the linear portion of a plot of the natural logarithm of cell number versus time, using the line fitting function of EXCEL. The results show that MCF7-0 cells grow better with the higher flow rate, and MDA-MB-231 cells grow better with a lower flow rate. Therefore, MDA-MB-231 cells seem to be more sensitive to media flow than MCF7-0 cells do. Based on this findings, all of the following experiment use a flow rate of 0.14 μ L/min for the growth of MCF7-0, and a flow rate of 0.05 μ L/min for the growth of MDA-MB-231cells.

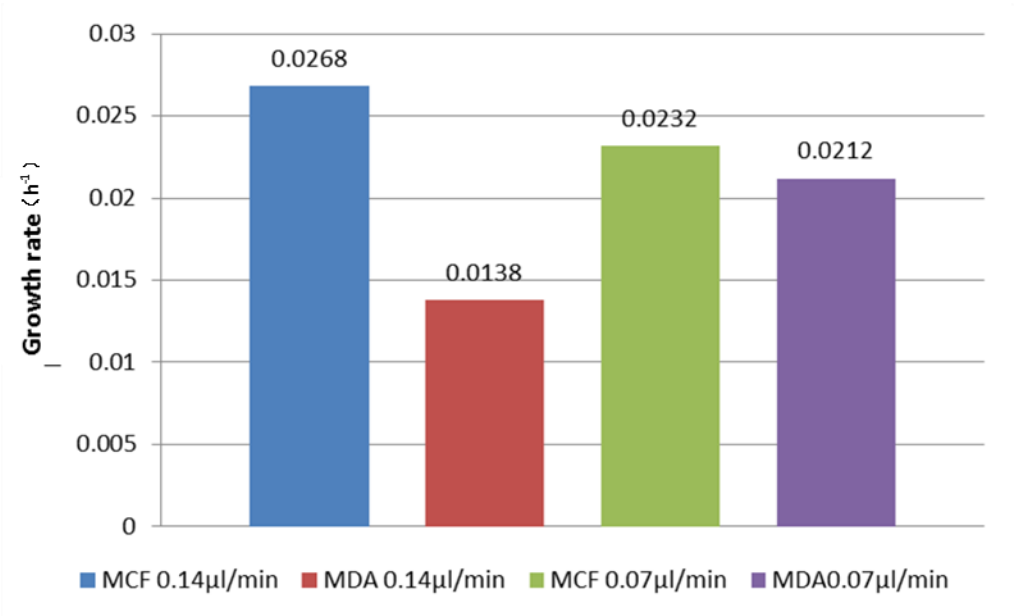

Figure 3.12 The effect of flow rate on cell culture with tumor-on-a-chip; The plot shows that MDA-MB-231 cells grow better under slower flow rate.

Metastatic potential between MCF7-0 and MDA-MB-231 cell lines under normoxia

MCF7-0 cells and MDA-MB-231 cells were cultured in tumor-on-a-chip device without gas flow to compare their metastatic potential. The migration channels were blocked with Matrigel. During a 52 hours culture, there are no MCF7-0 cells migrating through the migration channels while quite a lot of MDA-MB-231 cells, around 300 cells in average have migrated through the migration channels. (Figure3.13, Figure 3.14) Since the syringe pump could only been set at a single flow rate, the flow rate was set to 0.07 μ L/min. The device used for this study was on-chip designed device. Figure 3.12 shows the growth of both cell lines as well as the number of MDA-MB-231 cells that migrated. Three devices for each of the two cell lines were used. The number of cells that migrated cells among the three MDA-MB-231 cell loaded devices range from 117 to 909. Since the cells that have already traversed the migration channel to the circulatory channel would keep proliferating in that channel and cannot be distinguished during counting, the aggressiveness could be overestimated.

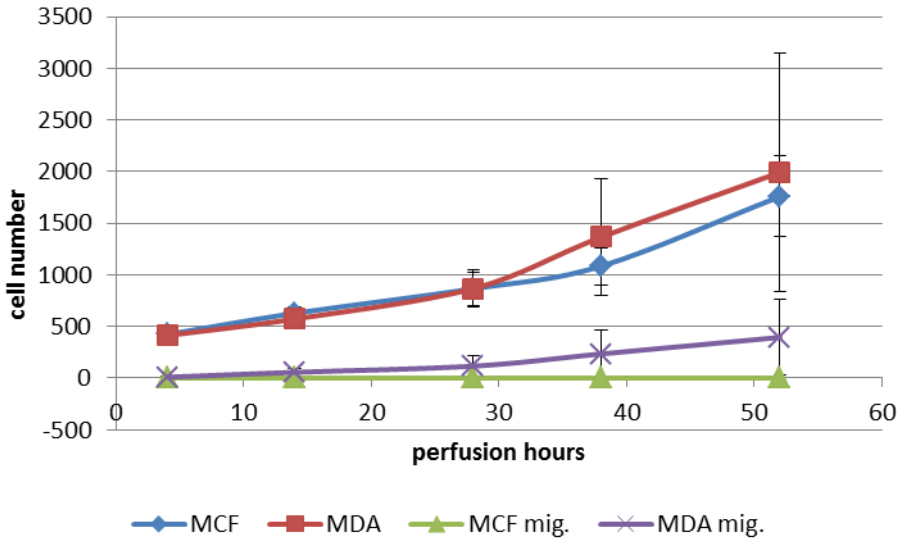

Figure 3.13 The comparison of aggressiveness between MCF7-0 and MDA-MB-231 cell line; There are around 300 MDA-MB-231 cells migrated in average during the 52 hours culture period, while no MCF7-0 cells traverse the migration channels.

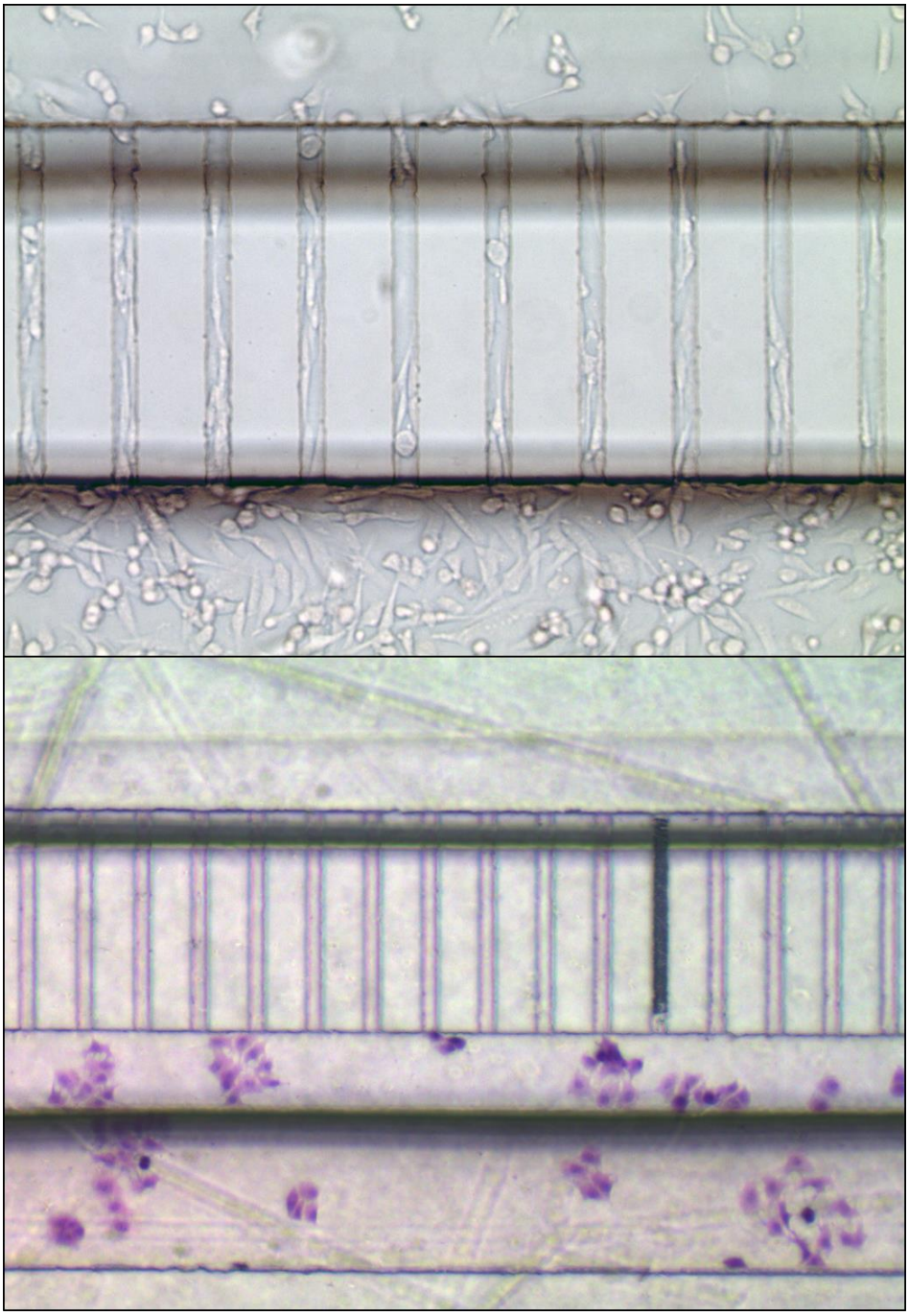

Figure 3.14 Photograph of MDA-MB-231 cells (top) and MCF7-0 cells (bottom, stained) growing in the device. MDA-MB-231 cells transvers the migration channels while MCF7-0 cells don't.

Comparison of growth rate between cells grow in the microfluidic device and in a standard tissue culture flask

The same passage of MCF7-0 cells were seeded into a microfluidic device and a standard polystyrene tissue culture flask to compare the growth rates. The flow rate in the device was set to 0.14 μ L/min. The cells from the same passage were seeded into ten T25 flasks with 87,000 cells per flask. Two of the flasks were trypsinized each day and the cells per flask were counted to generate the growth curve. The result shows that the grow rate of MCF7 cells cultured in tumor-on-a-chip device and that cultured in traditional cell culture flask are comparable (Figure 3.15). Since the cell number in tumor-on-a-chip device was counted by eye using the microscope, it would get harder when the cells grew to more than three thousand. As a result the count after 60 hours of perfusion may underscore the number of cells in the channel.

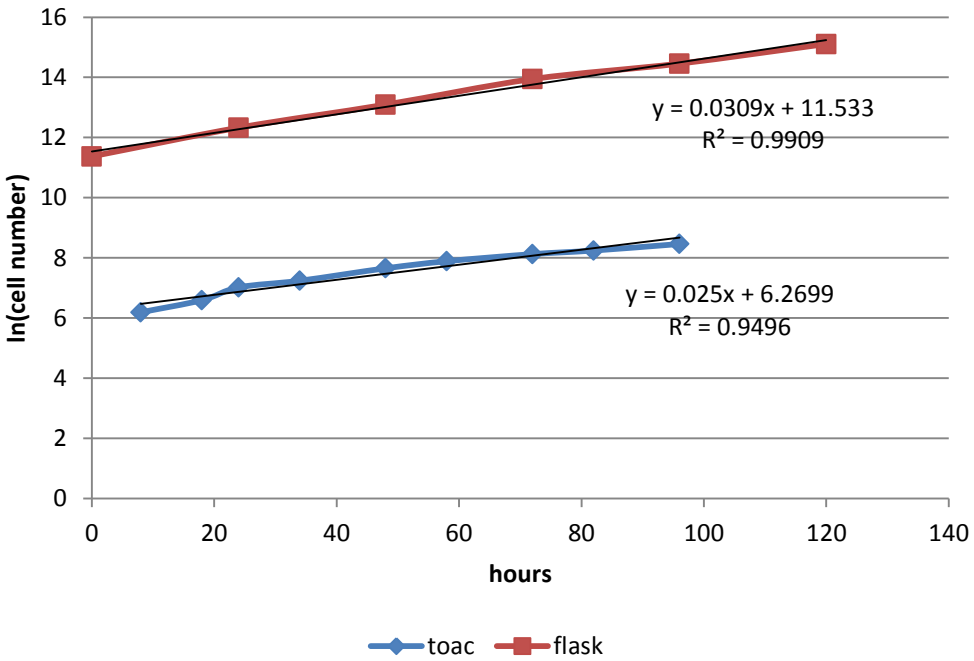

Figure 3.15 Comparison of cell growth in tumor-on-a-chip (toac) and in traditional cell culture flask; the growth rate is the slope of linear simulation of the cell growth curve.

3.4 Discussion

Our results show that both MDA-MB-231 and MCF7-0 breast cancer cell lines can be successfully cultured in this new tumor-on-a-chip device, with specific flow rates. With the migration channels blocked with a Matrigel barrier, the device stimulates the tumor microenvironment composed of a blood vessel and a basement membrane. The MDA-MB-231 cells successfully migrate through these migration channels in incubator air with no gas flow in the gas channel above the cell channels. The experiments using the device to culture cells under an oxygen gradient is still ongoing.

Culture of these two cell lines in our device shows that they have different resistance to media flow, in which MCF7-0 cells do better than MDA-MB-231 cells under flow. One possible explanation is that

MDA-MB-231 and MCF7-0 cells have different morphology when they attach to the glass substrate. MDA-MB-231 cells are more enlongated while MCF7-0 cells are often shaped as a polygon. As a result MDA-MB-231 cells may be exposed to more shear stress than MCF7-0 cells under equivalent flow. Numerous studies have used MDA-MB-231 and MCF-7 breast cancer cells to represent more and less aggressive breast cancer cell models with the MDA-MB-231 cells representing an aggressive cancer cell and the MCF-7 cells representing a less aggressive cancer cell[28]. Another possibility is that that MDA-MB-231 cells are known to be more aggressive and that may indicates that they may have fewer connecting proteins such as integrin to anchor them onto substrate, thus are easier to get flushed out of the channel at higher flow rates.

Another problem is the cells growing in the area where the hole is punched at the channel inlet in PDMS could deplete the nutrients in media. After cells are seeded in the device, there are still many cells remaining in the PDMS hole between channel inlet and reservoir of the on-top device, even after those left in reservoir have been washed off (Figure 3.16). These cells attach to the glass bottom below the reservoir and would compete for nutrients with cells downstream in the channel during

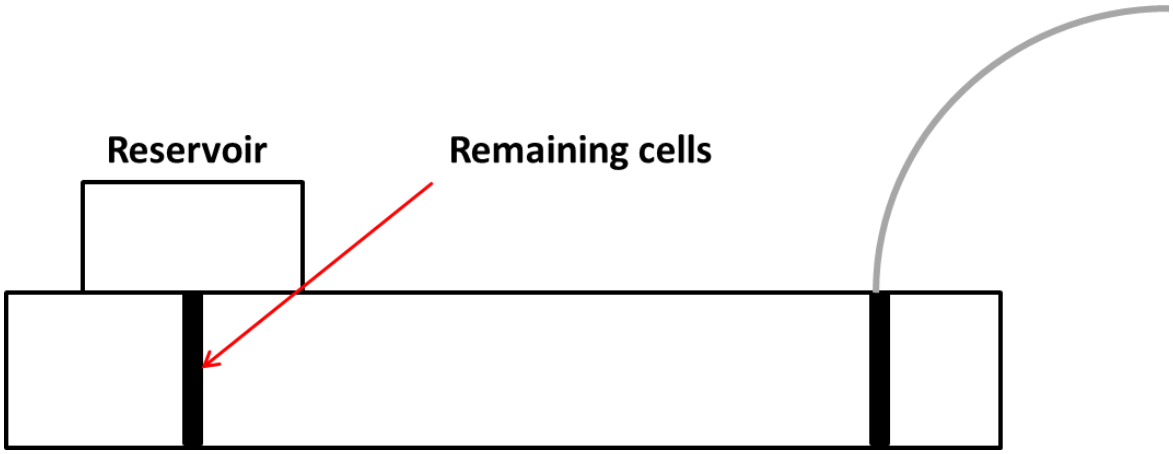

Figure 3.16 Diagram shows that cells remaining in the channel inlet after cell seeding

media perfusion. An approach to fix this problem could be silanizing the glass locally so that cells won't stick to that area, or introducing extra tubing in front of the entrance of the overlapped cell channel part. So that we can produce a U shape flow to flush the cells out of the hole area after cell seeding without disturbing those in channel (Figure 3.17).

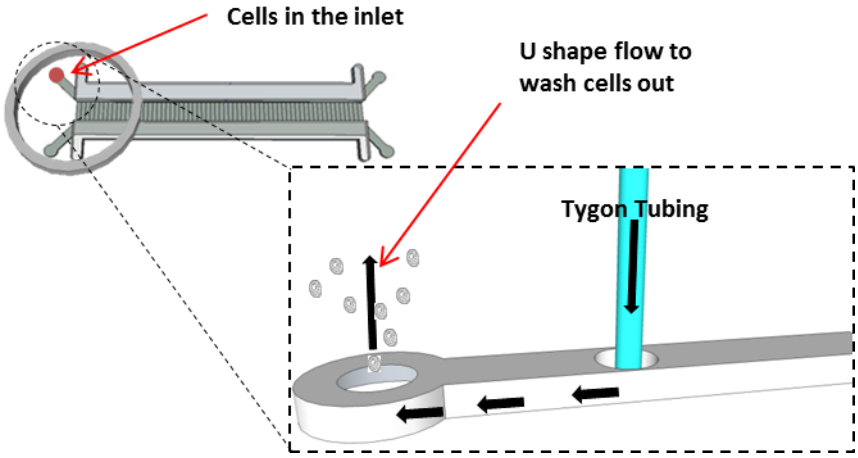

Figure 3.17 Diagram shows the introduction of a U shape flow to was the cells remained in the PDMS inlet after cell seeding,

The next step is to culture the two breast cancer cell lines under an oxygen gradient. Then, we can compare the aggressiveness of the cells with and without an oxygen gradient. Preliminary work has been done with MDA-MB-231 cells culturing in device under oxygen gradient. However, the growth rate of these cells is significantly slower than the control. Yet this is expected, for the cells have got used to culture under normoxia thus an oxygen level as low as 1% requires time for the cells to adapt. Even though the growth rate was slower, after five days under hypoxia a higher percentage of MDA-MB-231 cells migrated through the channel compared to these cells grown under the incubator atmosphere. There are about 50% MDA-MB-231 cells have traversed the migration channels in the device with oxygen gradient, while only around 10% MDA-MB-231 cells have in the device with incubator atmosphere. This indicates hypoxia increases the aggressiveness of the MDA-MB-231 cells. The experiment is still ongoing, to further confirm and explore the behavior of cells cultured under oxygen gradient.

Chapter 4. Conclusions

The work of this thesis concerns the development of microfluidic device that more accurately mimics the in vivo tumor microenvironment. The tumor-on-chip device functions as an invasion assay with Matrigel blocked channels and, at the same time, could control the temporal and spatial oxygen concentration. Thus, it enables us to model the cancer cell migration from its hypoxic, unstable microenvironment to the oxic environment of the circulatory system in a single, compact *in vitro* device. The work described in this thesis provides the first evidence to show that MDA-MB-231 and MCF7-0 breast cancer cells could be successfully cultured in tumor-on-a-chip device with media perfusion for a long term. Moreover, these cells show correspondent aggressive behavior by traversing the Matrigel blocked migration channels.

This work also determined the optimal flow rates to culture these two breast cancer cell lines. In the study of comparing different media delivery methods, the cell seeding method we use on off-chip reservoir device has been found to cause cell death downstream in channel. The exploration of its causes reveals that the cells trapped in the media delivery tubing could release substances toxic to cells. Indeed, the methods to set up a PDMS microfluidic cell culture system and to seed cells varies from study to study, but the biocompatible Tygon tubing is commonly used, and the situation described above may happen often in off-chip reservoir design. This may be able to explain why most studies use on-chip reservoirs to culture cells in PDMS microfluidic device. Our results provide a possible reason that using on-chip reservoir design is more successful in maintaining cell growth in microfluidic devices.

Much effort was spent in optimizing the steps for Matrigel filling of the migration channels in the tumor-on-a-chip device. The filling procedure is affected by the hydrophilicity of the device. Since the PDMS device is bonded to glass via plasma treating, the PDMS is temporarily made hydrophilic during this process. As time passes the PDMS surface reverts back to hydrophobic property and the Matrigel filling is more difficult. Moreover, Matrigel is a biological product, its protein content and character changes from batch to batch. Therefore, the filling efficiency would be unstable due to the variety of the Matrigel's surface tension and viscosity. To make the Matrigel filling process and also the master fabrication process

easier, our group are currently making a new design of the tumor-on-a-chip device. The migration channels are replaced with two lines of individual pillars. These pillars are separated with a specific distance thus form an unclosed channel for Matrigel. Ideally, the surface tension could hold the Matrigel at the front edge of the pillars. We also introduce an outlet and an inlet at the Matrigel channel so that the Matrigel can be filled directly, rather than by capillary effect as in the previous design. A newly designed device which contains pillars separated by 50 microns was tested and it shows promising result in Matrigel filling experiments. This new design can avoid the time-consuming 3D master fabrication step, Matrigel washing step, and can also study the path followed by cells when they migrate through the Matrigel, rather than likes that in the previous design where cells have a set migration path. Also in the future, we could put endothelia cells in the circulatory channel, which would make our device a more representative model for what happens in the tumor in *vivo*.

REFERENCES

Chapter 1

1. Aghi, M., Cohen, K. S., Klein, R. J., Scadden, D. T., and Chiocca, E. A. Tumor stromal-derived factor-1 recruits vascular progenitors to mitotic neovasculature, where microenvironment influences their differentiated phenotypes. *Cancer Research* 2006, 66(18), 9054-9064.

2. Albini, A., Iwamoto, Y., Kleinman, H. K., Martin, G. R., Aaronson, S. A., Kozlowski, J. M., and McEwan, R. N. A rapid in vitro assay for quantitating the invasive potential of tumor cells. *Cancer Research* 1987, 47(12), 3239-3245.

3. Al-Hajj, M., Wicha, M. S., Benito-Hernandez, A., Morrison, S. J., and Clarke, M. F. Prospective identification of tumorigenic breast cancer cells. *Proceedings of the National Academy of Sciences* 2003, 100(7), 3983-3988.

4. Allen, C. B., Schneider, B. K., and White, C. W. Limitations to oxygen diffusion and equilibration in in vitro cell exposure systems in hyperoxia and hypoxia. *American Journal of Physiology-Lung Cellular and Molecular Physiology* 2001, 281(4), L1021-L1027.

5. Al-Mehdi, A. B., Tozawa, K., Fisher, A. B., Shientag, L., Lee, A., and Muschel, R. J. Intravascular origin of metastasis from the proliferation of endothelium-attached tumor cells: a new model for metastasis. *Nature Medicine* 2000, 6(1), 100-102.

6. Ambrosio, G., Tritto, I., and Chiariello, M. The role of oxygen free radicals in preconditioning. *Journal of Molecular and Cellular Cardiology* 1995, 27(4), 1035-1039

7. Ambrosone C.B. Oxidants and antioxidants in breast cancer. Antioxid. *Redox Signal* 2000, 2: 903–917

8. American Cancer Society. Breast Cancer Facts and Figures 2011-2012. Atlanta: American Cancer Society, Inc.

9. Ao, M., Franco, O. E., Park, D., Raman, D., Williams, K., and Hayward, S. W. Cross-talk between paracrine-acting cytokine and chemokine pathways promotes malignancy in benign human prostatic epithelium. *Cancer Research* 2007, 67(9), 4244-4253.

10. Bae, Y. S., Sung, J. Y., Kim, O. S., Kim, Y. J., Hur, K. C., Kazlauskas, A., and Rhee, S. G. Platelet-derived growth factor-induced H2O2 production requires the activation of phosphatidylinositol 3-kinase. *Science Signaling* 2000, 275(14), 10527.

11. Barcellos-Hoff, M. H., and Ravani, S. A. Irradiated mammary gland stroma promotes the expression of tumorigenic potential by unirradiated epithelial cells. *Cancer Research* 2000, 60(5), 1254-1260.

12. Baumann, F., Leukel, P., Doerfelt, A., Beier, C. P., Dettmer, K., Oefner, P. J.,and Hau, P. Lactate promotes glioma migration by TGF-β2–dependent regulation of matrix metalloproteinase-2. *Neuro-oncology* 2009, 11(4), 368-380.

13. Beatty, G. L., and Paterson, Y. IFN-γ can promote tumor evasion of the immune system in vivo by down-regulating cellular levels of an endogenous tumor antigen. *The Journal of Immunology* 2000, 165(10), 5502-5508.

14. Benhar, M., Engelberg, D., and Levitzki, A. ROS, stress-activated kinases and stress signaling in cancer. *EMBO reports* 2002, 3(5), 420-425.

15. Bennewith, K. L., and Durand, R. E. Quantifying transient hypoxia in human tumor xenografts by flow cytometry. *Cancer Research* 2004, 64(17), 6183-6189.

16. Bensaad, K., and Vousden, K. H. Savior and slayer: the two faces of p53. *Nature Medicine* 2005, 11(12), 1278-1279.

17. Bergers, G., Brekken, R., McMahon, G., Vu, T. H., Itoh, T., Tamaki, K., and Hanahan, D. Matrix metalloproteinase-9 triggers the angiogenic switch during carcinogenesis. *Nature Cell Biology* 2000, 2(10), 737-744.

18. Bhowmick, N. A., Neilson, E. G., and Moses, H. L. Stromal fibroblasts in cancer initiation and progression. *Nature* 2004, 432(7015), 332-337.

19. Bissell, M. J., and Radisky, D. Putting tumours in context. *Nature Reviews Cancer* 2001, 1(1), 46-54.

20. Bonnet, D., and Dick, J. E. Human acute myeloid leukemia is organized as a hierarchy that originates from a primitive hematopoietic cell. *Nature Medicine* 1997, 3(7), 730-737.

21. Bonuccelli, G., Tsirigos, A., Whitaker-Menezes, D., Pavlides, S., Pestell, R. G., Chiavarina, B., and Lisanti, M. P. Ketones and lactate "fuel" tumor growth and metastasis: Evidence that epithelial cancer cells use oxidative mitochondrial metabolism. *Cell Cycle* 2010, 9(17), 3506-3514.

22. Bleul, C. C., Fuhlbrigge, R. C., Casasnovas, J. M., Aiuti, A., and Springer, T. A. A highly efficacious lymphocyte chemoattractant, stromal cell-derived factor 1 (SDF-1). *The Journal of Experimental Medicine* 1996, 184(3), 1101-1109.

23. Braun, R. D., Lanzen, J. L., and Dewhirst, M. W. Fourier analysis of fluctuations of oxygen tension and blood flow in R3230Ac tumors and muscle in rats. *American Journal of Physiology-Heart and Circulatory Physiology* 1999, 277(2), H551-H568.

24. Britta Weigelt, Johannes L. Peterse and Laura J. van't Veer. Breast Cancer Metastasis: Makers and Models, *Nature* 2005, 5: 591-602

25. Brizel DM, Rosner GL, Prosnitz LR and Dewhirst MW. Patterns and Variability of Tumor Oxygenation in Human Soft Tissue Sarcomas, Cervical Carcinomas, and lymph node metastases. *Int J Radiat Oncol Biol Phys* 1995, 32(4): 1121–1125.

26. Brown, L. F., Berse, B., Van De Water, L., Papadopoulos-Sergiou, A., Perruzzi, C. A., Manseau, E. J., and Senger, D. R. Expression and distribution of osteopontin in human tissues: widespread association with luminal epithelial surfaces. *Molecular Biology of the Cell* 1992, 3(10), 1169.

27. Bruna, A., Darken, R. S., Rojo, F., Ocaña, A., Peñuelas, S., Arias, A., and Seoane, J. High TGFβ-Smad activity confers poor prognosis in glioma patients and promotes cell proliferation depending on the methylation of the PDGF-B gene. *Cancer Cell* 2007, 11(2), 147-160.

28. Brurberg KG, Skogmo HK, Graff BA, Olsen DR, Rofstad EK. Fluctuations in pO2 in poorly and well-oxygenated spontaneous canine tumors before and during fractionated radiation therapy. *Radiother Oncol* 2005, 77: 220–6

29. Burdon, R. H. Superoxide and hydrogen peroxide in relation to mammalian cell proliferation. *Free Radical Biology and Medicine* 1995, 18(4), 775-794.

30. Buttke, T. M., Sandstrom, P. A. Oxidative stress as a mediator of apoptosis. *Immunology Today* 1994, 15(1), 7-10.

31. Cameron, M. D., Schmidt, E. E., Kerkvliet, N., Nadkarni, K. V., Morris, V. L., Groom, A. C., and MacDonald, I. C. Temporal progression of metastasis in lung: cell survival, dormancy, and location dependence of metastatic inefficiency. *Cancer Research* 2000, 60(9), 2541-2546.

32. Cairns, R. A., Kalliomaki, T., and Hill, R. P. Acute (cyclic) hypoxia enhances spontaneous metastasis of KHT murine tumors. *Cancer Research* 2001, 61(24), 8903-8908.

33. Cairns, R. A., Hill, R. P. Acute hypoxia enhances spontaneous lymph node metastasis in an orthotopic murine model of human cervical carcinoma. *Cancer Research* 2004, 64(6), 2054-2061.

34. Chaffer, C. L., and Weinberg, R. A. A perspective on cancer cell metastasis. *Science* 2011, 331(6024), 1559-1564.

35. Chambers, A. F., Groom, A. C., and MacDonald, I. C. Metastasis: dissemination and growth of cancer cells in metastatic sites. *Nature Reviews Cancer* 2002, 2(8), 563-572.

36. Chaplin, D. J., Durand, R. E., and Olive, P. L. Acute hypoxia in tumors: implications for modifiers of radiation effects. *International Journal of Radiation Oncology* Biology* Physics* 1986, 12(8), 1279-1282.

37. Chaw, K. C., Manimaran, M., Tay, E. H., and Swaminathan, S. Multi-step microfluidic device for studying cancer metastasis. *Lab on a Chip* 2007, 7(8), 1041-1047.

38. Chen, H. C. Boyden chamber assay. In *Cell Migration* 2005(pp. 15-22). Humana Press.

39. Cheng, G. C., Schulze, P. C., Lee, R. T., Sylvan, J., Zetter, B. R., and Huang, H. Oxidative stress and thioredoxin-interacting protein promote intravasation of melanoma cells. *Experimental Cell Research* 2004, 300(2), 297-307.

40. Cheng, S. Y., Heilman, S., Wasserman, M., Archer, S., Shuler, M. L., and Wu, M. A hydrogel-based microfluidic device for the studies of directed cell migration. *Lab on a Chip* 2007, 7(6), 763-769.

41. Christine L. Carter, Phd, Mph,Carol Allen, Phd,T and Donald E. Henson, Md. Relation of Tumor Size, Lymph Node Status, and Survival in 24,740 Breast Cancer Cases, *Cancer* 1989, 63: 181-187

42. Chung, S., Sudo, R., Mack, P. J., Wan, C. R., Vickerman, V., and Kamm, R. D. Cell migration into scaffolds under co-culture conditions in a microfluidic platform. *Lab on a Chip* 2009, 9(2), 269-275.

43. Clevers, H. The cancer stem cell: premises, promises and challenges. *Nature Medicine* 2011, 313-319.

44. Coussens, L. M., Raymond, W. W., Bergers, G., Laig-Webster, M., Behrendtsen, O., Werb, Z., and Hanahan, D. Inflammatory mast cells up-regulate angiogenesis during squamous epithelial carcinogenesis. *Genes and Development* 1999, 13(11), 1382-1397.

45. Coussens, L. M., Werb, Z. Inflammation and cancer. *Nature* 2002, 420(6917), 860-867.

46. Coussens, L. M., Werb, Z. Inflammatory Cells and Cancer Think Different!. *The Journal of Experimental Medicine* 2001, 193(6), F23-F26.

47. Dai, Y., Bae, K., Siemann, D. W. Impact of hypoxia on the metastatic potential of human prostate cancer cells. *International Journal of Radiation Oncology* Biology* Physics* 2011, 81(2), 521-528.

48. Dalerba, P., Dylla, S. J., Park, I. K., Liu, R., Wang, X., Cho, R. W., and Clarke, M. F. Phenotypic characterization of human colorectal cancer stem cells. *Proceedings of the National Academy of Sciences* 2007, 104(24), 10158-10163.

49. De Jaeger K, Kavanagh MC, Hill RP. Relationship of hypoxia to metastatic ability in rodent tumours. *Br. J. Cancer.* 2001, 84:1280–1285.

50. De Palma, M., Murdoch, C., Venneri, M. A., Naldini, L., and Lewis, C. E. Tie2-expressing monocytes: regulation of tumor angiogenesis and therapeutic implications. *Trends in Immunology* 2007, 28(12), 519-524.

51. Deng, G., Lu, Y., Zlotnikov, G., Thor, A. D., and Smith, H. S. Loss of heterozygosity in normal tissue adjacent to breast carcinomas. *Science* 1996, 274(5295), 2057-2059.

52. Derynck, R., Akhurst, R. J. Differentiation plasticity regulated by TGF-β family proteins in development and disease. *Nature Cell Biology* 2007, 9(9), 1000-1004.

53. Dewhirst, M. W., Braun, R. D., and Lanzen, J. L. Temporal changes in pO< sub> 2</sub> of R3230Ac tumors in fischer-344 rats. *International Journal of Radiation Oncology* Biology* Physics* 1998, 42(4), 723-726.

54. Dewhirst, M. W., Kimura, H., Rehmus, S. W., Braun, R. D., Papahadjopoulos, D., Hong, K., and Secomb, T. W. Microvascular studies on the origins of perfusion-limited hypoxia. *The British Journal of Cancer* 1996. Supplement, 27, S247.

55. Dewhirst, M. W. Intermittent hypoxia furthers the rationale for hypoxia-inducible factor-1 targeting. *Cancer Res* 2007, 67(3), 854-855.

56. Dontu, G., El-Ashry, D., and Wicha, M. S. Breast cancer, stem/progenitor cells and the estrogen receptor. *Trends in Endocrinology and Metabolism* 2004, 15(5), 193-197.

57. Fang, K. C., Wolters, P. J., Steinhoff, M., Bidgol, A., Blount, J. L., and Caughey, G. H. Mast cell expression of gelatinases A and B is regulated by kit ligand and TGF-β. *The Journal of Immunology* 1999, 162(9), 5528-5535.

58. Fearon, E. R., Vogelstein, B. Clonal analysis of human colorectal tumors. *Science* 1987, 238(4824), 193-197.

59. Fialkow, P. J. Clonal origin of human tumors. *Annual Review of Medicine* 1979, 30(1), 135-143.

60. Fidler, I. J. Metastasis: quantitative analysis distribution and fate of tumor emboli labeled with 125 I-5-iodo-2'-deoxyuridine, *J Natl Cancer Inst* 1970, 45: 773-782

61. Fidler, I. J. Selection of successive tumour lines for metastasis. *Nature* 1973, 242(118), 148-149.

62. Fidler, I. J., and Kripke, M. L. Metastasis results from preexisting variant cells within a malignant tumor. *Science* 1977, 197(4306), 893-895.

63. Fidler, I. J., and Hart, I. R. Biological diversity in metastatic neoplasms: origins and implications. *Science* 1982, 217(4564), 998-1003.

64. Fischer, K., Hoffmann, P., Voelkl, S., Meidenbauer, N., Ammer, J., Edinger, M., and Kreutz, M. Inhibitory effect of tumor cell–derived lactic acid on human T cells. *Blood* 2007, 109(9), 3812-3819.

65. Frame, S., Balmain, A. Integration of positive and negative growth signals during< i> ras</i> pathway activation< i> in vivo</i>. *Current Opinion in Genetics and Development* 2000, 10(1), 106-113.

66. Frank, B. T., Rossall, J. C., Caughey, G. H., and Fang, K. C. Mast cell tissue inhibitor of metalloproteinase-1 is cleaved and inactivated extracellularly by α-chymase. *The Journal of Immunology* 2001, 166(4), 2783-2792.

67. Friese, M. A., Wischhusen, J., Wick, W., Weiler, M., Eisele, G., Steinle, A., and Weller, M. RNA interference targeting transforming growth factor-β enhances NKG2D-mediated antiglioma immune response, inhibits glioma cell migration and invasiveness, and abrogates tumorigenicity in vivo. *Cancer Research* 2004, 64(20), 7596-7603.

68. Funamoto, K., Zervantonakis, I. K., Liu, Y., Ochs, C. J., Kim, C., and Kamm, R. D. A novel microfluidic platform for high-resolution imaging of a three-dimensional cell culture under a controlled hypoxic environment. *Lab on a Chip* 2012, 12(22), 4855-4863.

69. Furth, J., Kahn, M. C., Breedis, C. The transmission of leukemia of mice with a single cell. *The American Journal of Cancer* 1937, 31(2), 276-282.

70. Garber, K. Energy boost: the Warburg effect returns in a new theory of cancer. *Journal of the National Cancer Institute* 2004, 96(24), 1805-1806.

71. Garc á Olmo, D., Garcia Olmo, D. C., Ontanon, J., Martinez, E., and Vallejo, M. Tumor DNA circulating in the plasma might play a role in metastasis. *The Hypothesis of the Genometastasis. Histology and histopathology* 1999, 14(4), 1159-1164.

72. García-Olmo, D., García-Olmo, D. C., Ontañón, J., and Martinez, E. Horizontal transfer of DNA and the" genometastasis hypothesis". *Blood* 2000, 95(2), 724-725.

73. Gati, A., Guerra, N., Giron-Michel, J., Azzarone, B., Angevin, E., Moretta, A., and Caignard, A. Tumor cells regulate the lytic activity of tumor-specific cytotoxic T lymphocytes by modulating the inhibitory natural killer receptor function. *Cancer Research* 2001, 61(8), 3240-3244.

74. Ginestier, C., Hur, M. H., Charafe-Jauffret, E., Monville, F., Dutcher, J., Brown, M., and Dontu, G. ALDH1 is a marker of normal and malignant human mammary stem cells and a predictor of poor clinical outcome. *Cell Stem Cell* 2007, 1(5), 555-567.

75. Goetze, K., Walenta, S., Ksiazkiewicz, M., Kunz-Schughart, L. A., and Mueller-Klieser, W. Lactate enhances motility of tumor cells and inhibits monocyte migration and cytokine release. *International Journal of Oncology* 2010, 39(2), 453-463.

76. Gordan, J. D., Thompson, C. B., and Simon, M. C. HIF and c-Myc: sibling rivals for control of cancer cell metabolism and proliferation. *Cancer Cell* 2007, 12(2), 108-113

77. Gorelik, L., Flavell, R. A. Abrogation of TGFβ signaling in T cells leads to spontaneous T cell differentiation and autoimmune disease. *Immunity* 2000, 12(2), 171-181.

78. Gupta, A., Rosenberger, S. F., and Bowden, G. T. Increased ROS levels contribute to elevated transcription factor and MAP kinase activities in malignantly progressed mouse keratinocyte cell lines. *Carcinogenesis* 1999, 20(11), 2063-2073.

79. Guzy RD, Schumacker PT: Oxygen sensing by mitochondria at complex III: the paradox of increased reactive oxygen species during hypoxia. *Exp Physiol* 2006, 91:807-819

80. Halliwell, B. Oxidative stress and cancer: have we moved forward?. *Biochem. J* 2007, 401, 1-11.

81. Harris, J. F., Chambers, A. F., Hill, R. P., and Ling, V. Metastatic variants are generated spontaneously at a high rate in mouse KHT tumor. *Proceedings of the National Academy of Sciences* 1982, 79(18), 5547-5551.

82. Hattori, K., Heissig, B., Wu, Y., Dias, S., Tejada, R., Ferris, B., and Rafii, S. Placental growth factor reconstitutes hematopoiesis by recruiting VEGFR1+ stem cells from bone-marrow microenvironment. *Nature Medicine* 2002, 8(8), 841-849.

83. Heissig, B., Hattori, K., Dias, S., Friedrich, M., Ferris, B., Hackett, N. R., and Rafii, S. Recruitment of stem and progenitor cells from the bone marrow niche requires MMP-9 mediated release of kit-ligand. *Cell* 2002, 109(5), 625-637.

84. Heppner, G. H. Tumor heterogeneity. *Cancer Research* 1984, 44(6), 2259-2265.

85. Hess, K. R., Varadhachary, G. R., Taylor, S. H., Wei, W., Raber, M. N., Lenzi, R., and Abbruzzese, J. L. Metastatic patterns in adenocarcinoma. *Cancer* 2006, 106(7), 1624-1633.

86. Hirschhaeuser, F., Sattler, U. G., and Mueller-Klieser, W. Lactate: a metabolic key player in cancer. *Cancer Research* 2011, 71(22), 6921-6925.

87. Honn, K. V., Tang, D. G., Grossi, I., Duniec, Z. M., Timar, J., Renaud, C., and Marnett, L. J. Tumor cell-derived 12 (S)-hydroxyeicosatetraenoic acid induces microvascular endothelial cell retraction. *Cancer Research* 1994, 54(2), 565-574.

88. Hsieh, C. H., Chang, H. T., Shen, W. C., Shyu, W. C., and Liu, R. S. Imaging the impact of Nox4 in cycling hypoxia-mediated U87 glioblastoma invasion and infiltration. *Molecular Imaging and Biology* 2012, 14(4), 489-499.

89. Hsieh, C. H., Lee, C. H., Liang, J. A., Yu, C. Y., and Shyu, W. C. Cycling hypoxia increases U87 glioma cell radioresistance via ROS induced higher and long-term HIF-1 signal transduction activity. *Oncology Reports* 2010, 24(6), 1629-1636.

90. Huang, E. H., Heidt, D. G., Li, C. W., and Simeone, D. M. Cancer stem cells: a new paradigm for understanding tumor progression and therapeutic resistance. *Surgery* 2007, 141(4), 415-419.

91. Huang, Xiaowen, Li Li, Qin Tu, Jianchun Wang, Wenming Liu, Xueqin Wang, Li Ren, and Jinyi Wang. On-chip cell migration assay for quantifying the effect of ethanol on MCF-7 human breast cancer cells. *Microfluidics and Nanofluidics* 2011, 10(6), 1333-1341.

92. Irimia, D., Charras, G., Agrawal, N., Mitchison, T., and Toner, M. Polar stimulation and constrained cell migration in microfluidic channels. *Lab on a Chip* 2007, 7(12), 1783-1790.

93. Jennings, M. T., and Pietenpol, J. A. The role of transforming growth factor β in glioma progression. *Journal of Neuro-oncology* 1998, 36(2), 123-140.

94. Jessup JM, Battle P, Waller H, Edmiston KH, Stolz DB, Watkins SC, Locker J, Skena K. Reactive nitrogen and oxygen radicals formed during hepatic ischemia-reperfusion kill weakly metastatic colorectal cancer cells. *Cancer Res* 1999; 59: 1825-1829

95. Kaelin Jr, William G. The von Hippel–Lindau tumour suppressor protein: O2 sensing and cancer. *Nature Reviews Cancer* 2008, 8(11): 865-873

96. Kakarala, M., Wicha, M. S. Implications of the cancer stem-cell hypothesis for breast cancer prevention and therapy. *Journal of Clinical Oncology* 2008, 26(17), 2813-2820.

97. Karnoub, A. E., Dash, A. B., Vo, A. P., Sullivan, A., Brooks, M. W., Bell, G. W., and Weinberg, R. A. Mesenchymal stem cells within tumour stroma promote breast cancer metastasis. *Nature* 2007, 449(7162), 557-563.

98. Kawaguchi, T., Nakamura, K. Analysis of the lodgement and extravasation of tumor cells in experimental models of hematogenous metastasis. *Cancer and Metastasis Reviews* 1986, 5(2), 77-94.

99. Kerbel, R. S., Waghorne, C., Man, M. S., Elliott, B., and Breitman, M. L. Alteration of the tumorigenic and metastatic properties of neoplastic cells is associated with the process of calcium phosphate-mediated DNA transfection. *Proceedings of the National Academy of Sciences* 1987, 84(5), 1263-1267.

100. Kerbel, R. S., Waghorne, C., Korczak, B., Lagarde, A., and Breitman, M. L. Clonal dominance of primary tumours by metastatic cells: genetic analysis and biological implications. *Cancer Surveys* 1987, 7(4), 597-629.

101. Kim, Y. M., Kim, K. E., Koh, G. Y., Ho, Y. S., and Lee, K. J. Hydrogen peroxide produced by angiopoietin-1 mediates angiogenesis. *Cancer Research* 2006, 66(12), 6167-6174.

102. Kim, J. W., Dang, C. V. Cancer's molecular sweet tooth and the Warburg effect. *Cancer Research* 2006, 66(18), 8927-8930.

103. Klaunig JE, Xu Y, Isenberg JS, Bachowski S, Kolaja KL, Jiang J, Stevenson DE, Walborg EF, Jr. The role of oxidative stress in chemical carcinogenesis. *Environ. Health Perspect* 1998; 106(Suppl 1): 289–295

104. Kalliomaki TM, McCallum G, Lunt SJ, Wells PG, Hill RP. Analysis of the effects of exposure to acute hypoxia on oxidative lesions and tumour progression in a transgenic mouse breast cancer model. *BMC Cancer.* 2008, 8:151.

105. Kalliomaki TM, McCallum G, Wells PG, Hill RP. Progression and metastasis in a transgenic mouse breast cancer model: effects of exposure to in vivo hypoxia. *Cancer Lett*. 2009, 282:98–108

106. Klimova, T., N. S. Chandel. Mitochondrial complex III regulates hypoxic activation of HIF. *Cell Death and Differentiation* 2008,15 (4): 660-666

107.Kundu, N., Zhang, S., and Fulton, A. M. Sublethal oxidative stress inhibits tumor cell adhesion and enhances experimental metastasis of murine mammary carcinoma. *Clinical and Experimental Metastasis* 1995, 13(1), 16-22.

108.Lam, R. H., Kim, M. C., and Thorsen, T. Culturing aerobic and anaerobic bacteria and mammalian cells with a microfluidic differential oxygenator. *Analytical Chemistry* 2007, 81(14), 5918-5924.

109. Langley, R. R., Fidler, I. J. The seed and soil hypothesis revisited—The role of tumor‐stroma interactions in metastasis to different organs. *International Journal of Cancer* 2011, 128(11), 2527-2535.

110.Lanzen J, Braun RD, Klitzman B, Brizel D, Secomb TW, Dewhirst MW. Direct demonstration of instabilities in oxygen concentrations within the extravascular compartment of an experimental tumor. *Cancer Res* 2006, 66: 2219–23

111. Lapidot, T., Sirard, C., Vormoor, J., Murdoch, B., Hoang, T., Caceres-Cortes, J., and Dick, J. E. A cell initiating human acute myeloid leukaemia after transplantation into SCID mice. *Nature* 1994, 367: 645-648

112. Leighton, J. Inherent malignancy of cancer cells possibly limited by genetically differing cells in the same tumour. *Acta Cytol* 1965, 9, 138-140.

113.Li, Y. H., Zhu, C. A modified Boyden chamber assay for tumor cell transendothelial migration in vitro. *Clinical and Experimental Metastasis* 1999, 17(5), 423-429.

114. Lin, E. Y., Nguyen, A. V., Russell, R. G., and Pollard, J. W. Colony-stimulating factor 1 promotes progression of mammary tumors to malignancy. *The Journal of Experimental Medicine* 2001, 193(6), 727-740.

115. Ling, V., Chambers, A. F., Harris, J. F., and Hill, R. P. Quantitative genetic analysis of tumor progression. *Cancer and Metastasis Reviews* 1985, 4(2), 173-192.

116. Ling, L. J., Wang, S., Liu, X. A., Shen, E. C., Ding, Q., Lu, C., and Wang, F. A novel mouse model of human breast cancer stem-like cells with high CD44+ CD24-/lower phenotype metastasis to human bone. *Chin Med J (Engl)* 2008, 121(20), 1980-1986.

117.Lo, J. F., Sinkala, E., and Eddington, D. T. Oxygen gradients for open well cellular cultures via microfluidic substrates. *Lab on a Chip* 2010, 10(18), 2394-2401.

118. Lundgren K, Holm C and Landberg G. Hypoxia and Breast Cancer: prognostic and therapeutic implications. *Cell Mol Life Sci* 2007, 64: 3233-3247

119. Luzzi, K. J., MacDonald, I. C., Schmidt, E. E., Kerkvliet, N., Morris, V. L., Chambers, A. F., and Groom, A. C. Multistep nature of metastatic inefficiency: dormancy of solitary cells after successful extravasation and limited survival of early micrometastases. *The American Journal of Pathology* 1998, 153(3), 865-873.

120. Majmundar, Amar J., Waihay J. Wong, and M. Celeste Simon. Hypoxia-inducible factors and the response to hypoxic stress. *Molecular Cell* 2010, 40(2): 294-309

121. Makino, S. Further evidence favoring the concept of the stem cell in ascites tumors of rats. *Annals of the New York Academy of Sciences* 1956, 63(5), 818-830.

122. Manuela Milani, Adrian L. Harris. Targeting Tumour Hypoxia in Breast Cancer, European Journal Of *Cancer* 2008, 44: 2766-2773

123. Moldovan, L., Irani, K., Moldovan, N. I., Finkel, T., and Goldschmidt-Clermont, P. J. The actin cytoskeleton reorganization induced by Rac1 requires the production of superoxide. *Antioxidants and Redox Signaling* 1999, 1(1), 29-43.

124. Muir, D., Sukhu, L., Johnson, J., Lahorra, M. A., and Maria, B. L. Quantitative methods for scoring cell migration and invasion in filter-based assays. *Analytical Biochemistry* 1993, 215(1), 104-109.

125. Nelson, K. K., Melendez, J. A. Mitochondrial redox control of matrix metalloproteinases. *Free Radical Biology and Medicine* 2004, 37(6), 768-784.

126. "Non-inasive or Invasive Breast Cancer." BREASTCANCER.ORG. Breastcancer.org, 19 Sept. 2012. Web. 16 Apr. 2013. http://www.breastcancer.org/symptoms/diagnosis/invasive

127. Newell, K., Franchi, A., Pouysségur, J., and Tannock, I. Studies with glycolysis-deficient cells suggest that production of lactic acid is not the only cause of tumor acidity. *Proceedings of the National Academy of Sciences* 1993, 90(3), 1127-1131.

128. Nowell, P. C.A minute chromosome in human chronic granulocytic leukemia. *Science* 1960, 132, 1497.

129. O'Brien, C. A., Pollett, A., Gallinger, S., and Dick, J. E. A human colon cancer cell capable of initiating tumour growth in immunodeficient mice. *Nature* 2006, 445(7123), 106-110.

130. Oppegard, S. C., Nam, K. H., Carr, J. R., Skaalure, S. C., and Eddington, D. T. Modulating temporal and spatial oxygenation over adherent cellular cultures. *PloS One* 2009, 4(9), e6891.

131. Parkins, C. S., Dennis, M. F., Stratford, M. R., Hill, S. A., and Chaplin, D. J. Ischemia reperfusion injury in tumors: the role of oxygen radicals and nitric oxide. *Cancer Research* 1995, 55(24), 6026-6029.

132. Pavlides, S., Whitaker-Menezes, D., Castello-Cros, R., Flomenberg, N., Witkiewicz, A. K., Frank, P. G., and Lisanti, M. P. The reverse Warburg effect: aerobic glycolysis in cancer associated fibroblasts and the tumor stroma. *Cell Cycle* 2009, 8(23), 3984-4001.

133. Payne, S. L., Fogelgren, B., Hess, A. R., Seftor, E. A., Wiley, E. L., Fong, S. F., and Kirschmann, D. A. Lysyl oxidase regulates breast cancer cell migration and adhesion through a hydrogen peroxide–mediated mechanism. *Cancer Research* 2005, 65(24), 11429-11436.

134. Peinado, H., Lavotshkin, S., and Lyden, D. The secreted factors responsible for pre-metastatic niche formation: old sayings and new thoughts. In Seminars in cancer biology (Vol. 21, No. 2, pp. 139-146). *Academic Press* 2011.

135. Petros, J. A., Baumann, A. K., Ruiz-Pesini, E., Amin, M. B., Sun, C. Q., Hall, J., and Wallace, D. C. mtDNA mutations increase tumorigenicity in prostate cancer. *Proceedings of the National Academy of Sciences of the United States of America* 2005, 102(3), 719-724.

136. Phillips, T. M., McBride, W. H., and Pajonk, F. The response of CD24−/low/CD44+ breast cancer–initiating cells to radiation. *Journal of the National Cancer Institute* 2006, 98(24), 1777-1785.

137. Pierce, G. B., Wallace, C. Differentiation of malignant to benign cells. *Cancer Research* 1971, 31(2), 127-134.

138. Pierce, G. B., Speers, W. C. Tumors as caricatures of the process of tissue renewal: prospects for therapy by directing differentiation. *Cancer Research* 1988, 48(8), 1996-2004.

139. Preston, T. J., Muller, W. J., and Singh, G. Scavenging of extracellular H2O2 by catalase inhibits the proliferation of HER-2/Neu-transformed rat-1 fibroblasts through the induction of a stress response. *Journal of Biological Chemistry* 2001, 276(12), 9558-9564.

140. Qian, B., Deng, Y., Im, J. H., Muschel, R. J., Zou, Y., Li, J., and Pollard, J. W. A distinct macrophage population mediates metastatic breast cancer cell extravasation, establishment and growth. *PLoS One* 2009, 4(8), e6562.

141. Quintana, E., Shackleton, M., Sabel, M. S., Fullen, D. R., Johnson, T. M., and Morrison, S. J. Efficient tumour formation by single human melanoma cells. *Nature* 2008, 456(7222), 593-598.

142. Quintana, Elsa Mark Shackleton, Hannah R. Foster, Douglas R. Fullen, Michael S. Sabel, Timothy M. Johnson, and Sean J. Morrison. "Phenotypic heterogeneity among tumorigenic melanoma cells from patients that is reversible and not hierarchically organized." *Cancer Cell* 2010, 18 (5): 510-523.

143. Rajagopalan, S., Meng, X. P., Ramasamy, S., Harrison, D. G., and Galis, Z. S. Reactive oxygen species produced by macrophage-derived foam cells regulate the activity of vascular matrix metalloproteinases in vitro. Implications for atherosclerotic plaque stability. *Journal of Clinical Investigation* 1996, 98(11), 2572.

144. Reya, T., Morrison, S. J., Clarke, M. F., and Weissman, I. L. Stem cells, cancer, and cancer stem cells. *Nature* 2001, 414(6859), 105-111.

145. Ricci-Vitiani, L., Lombardi, D. G., Pilozzi, E., Biffoni, M., Todaro, M., Peschle, C., and De Maria, R. Identification and expansion of human colon-cancer-initiating cells. *Nature* 2006, 445(7123), 111-115.

146. Rodriguez, L. G., Wu, X., and Guan, J. L. Wound-healing assay. In *Cell Migration* 2005 (pp. 23-29). Humana Press.

147. Rofstad EK, Galappathi K, Mathiesen B, Ruud EB. Fluctuating and diffusion-limited hypoxia in hypoxia-induced metastasis. *Clin. Cancer Res.* 2007, 13:1971–1978.

148. Ronnov-Jessen, L., Petersen, O. W., and Bissell, M. J. Cellular changes involved in conversion of normal to malignant breast: importance of the stromal reaction. *Physiological Reviews* 1996, 76(1), 69-125.

149. Rosenthal, E., McCrory, A., Talbert, M., Young, G., Murphy‐Ullrich, J., and Gladson, C. Elevated expression of TGF‐β1 in head and neck cancer‐associated fibroblasts. *Molecular Carcinogenesis* 2004, 40(2), 116-121.

150. Sakariassen, P. Ø., Immervoll, H., and Chekenya, M Cancer stem cells as mediators of treatment resistance in brain tumors: status and controversies. *Neoplasia (New York, NY)* 2007, 9(11), 882.

151. Schmidt, S. M., Schag, K., Müller, M. R., Weck, M. M., Appel, S., Kanz, L., and Brossart, P. Survivin is a shared tumor-associated antigen expressed in a broad variety of malignancies and recognized by specific cytotoxic T cells. *Blood* 2003, 102(2), 571-576.

152. Schumacker, P. T. Reactive oxygen species in cancer cells: live by the sword, die by the sword. *Cancer Cell* 2006, 10(3), 175-176.

153. Secomb, T. W., Hsu, R., Dewhirst, M. W., Klitzman, B., and Gross, J. F. Analysis of oxygen transport to tumor tissue by microvascular networks. *International Journal of Radiation Oncology* Biology* Physics* 1993, 25(3), 481-489.

154. Semenza, Gregg. L. HIF-1: upstream and downstream of cancer metabolism. *Current Opinion in Genetics and Development*, 2010, 20(1), 51-56

155. Shackleton, M., Quintana, E., Fearon, E. R., and Morrison, S. J. Heterogeneity in cancer: cancer stem cells versus clonal evolution. *Cell* 2009, 138(5), 822-829.

156. Shimoda, M., Mellody, K. T., and Orimo, A. Carcinoma-associated fibroblasts are a rate-limiting determinant for tumour progression. In Seminars in cell and developmental biology 2010(Vol. 21, No. 1, pp. 19-25). *Academic Press*.

157. Shmelkov, S. V., Butler, J. M., Hooper, A. T., Hormigo, A., Kushner, J., Milde, T., and Rafii, S. CD133 expression is not restricted to stem cells, and both CD133+ and CD133–metastatic colon cancer cells initiate tumors. *The Journal of Clinical Investigation* 2008, 118(6), 2111.

158. Sia, S. K., Whitesides, G. M. Microfluidic devices fabricated in poly (dimethylsiloxane) for biological studies. *Electrophoresis* 2003, 24(21), 3563-3576.

159. Singh, S. K., Hawkins, C., Clarke, I. D., Squire, J. A., Bayani, J., Hide, T., and Dirks, P. B. Identification of human brain tumour initiating cells. *Nature* 2004, 432(7015), 396-401.

160. Sieuwerts, A. M., Klijn, J. G., and Foekens, J. A. Assessment of the invasive potential of human gynecological tumor cell lines with the in vitro Boyden chamber assay: influences of the ability of cells to migrate through the filter membrane. *Clinical and Experimental Metastasis* 1997, 15(1), 53-62.

161. Sorg BS, Moeller BJ, Donovan O, Cao Y, Dewhirst MW. Hyperspectral imaging of hemoglobin saturation in tumor microvasculature and tumor hypoxia development. *J Biomed Opt* 2005, 10: 44004.

162. Stackpole, C. W. Distinct lung-colonizing and lung-metastasizing cell populations in B16 mouse melanoma. *Nature* 1981, 298,798-80

163. "Stages of Breast Cancer." BREASTCANCER.ORG. Breastcancer.org, 19 Sept. 2012. Web. 16 Apr. 2013. http://www.breastcancer.org/symptoms/diagnosis/stages

164. Subarsky P, Hill RP. Graded hypoxia modulates the invasive potential of HT1080 fibrosarcoma and MDA MB231 carcinoma cells. *Clin Exp Metastasis* 2008; 25: 253-264

165. Thiery, J. P. Epithelial–mesenchymal transitions in development and pathologies. *Current Opinion in Cell Biology* 2003, 15(6), 740-746.

166. Thiery, J. P., Acloque, H., Huang, R. Y., and Nieto, M. A. Epithelial-mesenchymal transitions in development and disease. *Cell* 2009, 139(5), 871-890.

167. Thomas, D. A., Massagué, J. TGF-β directly targets cytotoxic T cell functions during tumor evasion of immune surveillance. *Cancer Cell* 2005, 8(5), 369-380.

168. T. Gohongi, D. Fukumura, Y. Boucher, C.O. Yun, G.A. Soff, C. Compton, T. Todoroki, R.K. Jain. Tumor-host interactions in the gallbladder suppress distal angiogenesis and tumor growthinvolvement of transforming growth factor beta1. *Nat. Med.*1999, 5: 1203–1208

169. Ushio-Fukai, M. Redox signaling in angiogenesis: role of NADPH oxidase. *Cardiovascular Research* 2006, 71(2), 226-235.

170. Vaage, J. Metastasizing potentials of mouse mammary tumors and their metastases. *International Journal of Cancer* 1988, 41(6), 855-858.

171. Van der Meer, A. D., Vermeul, K., Poot, A. A., Feijen, J., and Vermes, I. A microfluidic wound-healing assay for quantifying endothelial cell migration. *American Journal of Physiology-Heart and Circulatory Physiology* 2010, 298(2), H719-H725.

172. Van Wetering, S., van Buul, J. D., Quik, S., Mul, F. P., Anthony, E. C., ten Klooster, J. P., and Hordijk, P. L. Reactive oxygen species mediate Rac-induced loss of cell-cell adhesion in primary human endothelial cells. *Journal of Cell Science* 2002, 115(9), 1837-1846.

173. Vaupel P, Hockel M, Mayer A. Detection and Characterization of Tumor Hypoxia Using pO_2 Histography. *Antioxid Redox Signal* 2007, 9(8): 1221–1235.

174. Vogelstein, B., Kinzler, K. W. Cancer genes and the pathways they control. *Nature Medicine* 2004, 10(8), 789-799.

175. Walenta, S., Wetterling, M., Lehrke, M., Schwickert, G., Sundfør, K., Rofstad, E. K., and Mueller-Klieser, W. High lactate levels predict likelihood of metastases, tumor recurrence, and restricted patient survival in human cervical cancers. *Cancer Research* 2000, 60(4), 916-921.

176. Walenta, S., and Mueller-Klieser, W. F. Lactate: mirror and motor of tumor malignancy. In Seminars in radiation oncology 2004 (Vol. 14, No. 3, pp. 267-274). WB Saunders.

177. Wang, L., Zhu, J., Deng, C., Xing, W. L., and Cheng, J. An automatic and quantitative on-chip cell migration assay using self-assembled monolayers combined with real-time cellular impedance sensing. *Lab on a Chip* 2008, 8(6), 872-878.

178. Weigelt, B., Peterse, J. L., and van't Veer, L. J. Breast cancer metastasis: markers and models. *Nature Reviews Cancer* 2005, 5(8), 591-602.

179. Weitzman, S. A., Weitberg, A. B., Clark, E. P., and Stossel, T. P. Phagocytes as carcinogens: malignant transformation produced by human neutrophils. *Science* 1985, 227(4691), 1231-1233.

180. Wiseman, H., Kaur, H., and Halliwell, B. DNA damage and cancer: measurement and mechanism. *Cancer Letters* 1995, 93(1), 113-120.

181. Wiseman, H., and Halliwell, B. Damage to DNA by reactive oxygen and nitrogen species: role in inflammatory disease and progression to cancer. *Biochem* 1996. J, 313, 17-29.

182. Wong, Carmen Chak-Lui, Daniele M. Gilkes, Huafeng Zhang, Jasper Chen, Hong Wei, Pallavi Chaturvedi, Stephanie I. Fraley, Hypoxia-inducible factor 1 is a master regulator of breast cancer metastatic niche formation. *Proceedings of the National Academy of Sciences* 2011, 108(39): 16369-16374.

183. Yabu, M., Shime, H., Hara, H., Saito, T., Matsumoto, M., Seya, T. and Inoue, N. IL-23-dependent and-independent enhancement pathways of IL-17A production by lactic acid. *International Immunology* 2010, 23(1), 29-41.

184. Yachida, S., Jones, S., Bozic, I., Antal, T., Leary, R., Fu, B., and Iacobuzio-Donahue, C. A. Distant metastasis occurs late during the genetic evolution of pancreatic cancer. *Nature* 2010, 467(7319), 1114-1117.

185. Yamaura, H., and Matsuzawa, T. Tumour regrowth after irradiation: an experimental approach. *International Journal of Radiation Biology* 1979, 35(3), 201-219.

186. Yoshikawa, T., Kokura, S., Oyamada, H., Iinuma, S., Nishimura, S., Kaneko, T., and Kondo, M. Antitumor effect of ischemia-reperfusion injury induced by transient embolization. *Cancer Research* 1994, 54(19), 5033-5035.

187. Ziebart, T., Walenta, S., Kunkel, M., Reichert, T. E., Wagner, W., and Mueller-Klieser, W. Metabolic and proteomic differentials in head and neck squamous cell carcinomas and normal gingival tissue. *Journal of Cancer Research and Clinical Oncology* 2011, 137(2), 193-199.

Chapter 2

1. Bonuccelli, G., Tsirigos, A., Whitaker-Menezes, D., Pavlides, S., Pestell, R. G., Chiavarina, B., and Lisanti, M. P. Ketones and lactate "fuel" tumor growth and metastasis: Evidence that epithelial cancer cells use oxidative mitochondrial metabolism. *Cell Cycle* 2010, 9(17), 3506-3514.

2. Chen, Development of Microfluidic Devices for Long-term Cell Culture and High-Throughput Clonal Analysis (Doctoral dissertation, The University of New South Wales).2012

3. Goetze, K., Walenta, S., Ksiazkiewicz, M., Kunz-Schughart, L. A., and Mueller-Klieser, W. Lactate enhances motility of tumor cells and inhibits monocyte migration and cytokine release. *International Journal of Oncology* 2011, 39(2), 453-463.

4. Kim, L., Toh, Y. C., Voldman, J., and Yu, H. A practical guide to microfluidic perfusion culture of adherent mammalian cells. *Lab on a Chip* 2007, 7(6), 681-694.

5. Kim, L. Y. Microfluidic perfusion culture for controlling the stem cell microenvironment (Doctoral dissertation, Massachusetts Institute of Technology).2008

6. Martinez-Outschoorn, U. E., Prisco, M., Ertel, A., Tsirigos, A., Lin, Z., Pavlides, S., and Lisanti, M. P. Ketones and lactate increase cancer cell "stemness," driving recurrence, metastasis and poor clinical outcome in breast cancer: achieving personalized medicine via Metabolo-Genomics. *Cell Cycle* 2011, 10(8), 1271-1286.

7. Su, X., Theberge, A. B., January, C. T., and Beebe, D. J. Effect of Microculture on Cell Metabolism and Biochemistry: Do Cells Get Stressed in Microchannels?. *Analytical Chemistry* 2013, 85(3), 1562-1570.

8. Yamamoto, K., Sokabe, T., Watabe, T., Miyazono, K., Yamashita, J. K., Obi, S., and Ando, J. Fluid shear stress induces differentiation of Flk-1-positive embryonic stem cells into vascular endothelial cells in vitro. *American Journal of Physiology-Heart and Circulatory Physiology* 2005, 288(4), H1915-H1924.

9. Sung, J. H., Shuler, M. L. Prevention of air bubble formation in a microfluidic perfusion cell culture system using a microscale bubble trap. *Biomedical Microdevices* 2009, 11(4), 731-738.

10. Alfarouk, K. O., Muddathir, A. K., and Shayoub, M. E. Tumor acidity as evolutionary spite. *Cancers* 2011, 3(1), 408-414.

Chapter 3

1. Adler M, Polinkovsky M, Gutierrez E, Groisman A. Generation of oxygen gradients with arbitrary shapes in a microfluidic device. *Lab Chip* 2010; 10: 388-391.

2. Braun, R. D., Lanzen, J. L., and Dewhirst, M. W. Fourier analysis of fluctuations of oxygen tension and blood flow in R3230Ac tumors and muscle in rats. *American Journal of Physiology-Heart and Circulatory Physiology* 1999, 277(2), H551-H568.

3. Cairns RA, Hill RP. Acute hypoxia enhances spontaneous lymph node metastasis in an orthotopic murine model of human cervical carcinoma. *Cancer Res* 2004; 64: 2054-2061.

4. Chaw KC, Manimaran M, Tay FEH, Swaminathan S. A quantitative observation and imaging of single tumor cell migration and deformation using a multi-gap microfluidic device representin the blood vessel. *Microvasc Res* 2006; 72: 153-160.

5. Chaw KC, Manimaran M, Tay EH, Swaminathan S. Multi-step microfluidic device for studying cancer metastasis. *Lab Chip* 2007; 7: 1041-1047.

6. Dai Y, Bae K, Siemann DW. Impact of hypoxia on the metatatic potential of human prostate cancer cells. *Int J Radiat Oncol Biol Phys* 2011; 81: 521-528

7. Dewhirst, M. W., Cao, Y., and Moeller, B. Cycling hypoxia and free radicals regulate angiogenesis and radiotherapy response. *Nature Reviews Cancer* 2008, 8(6), 425-437.

8. Hill RP, Marie-Egyptienne DT, Hedley DW. Cancer stem cells, hypoxia and metastasis. *Semin Radiat Oncol* 2009; 19: 106-111.

9. Hsieh, C. H., Chang, H. T., Shen, W. C., Shyu, W. C., and Liu, R. S. Imaging the impact of Nox4 in cycling hypoxia-mediated U87 glioblastoma invasion and infiltration. *Molecular Imaging and Biology* 2012, 14(4), 489-499.

10. Jessup JM, Battle P, Waller H, Edmiston KH, Stolz DB, Watkins SC, Locker J, Skena K. Reactive nitrogen and oxygen radicals formed during hepatic ischemia-reperfusion kill weakly metastatic colorectal cancer cells. *Cancer Res* 1999; 59: 1825-1829.

11. Kim HJ, Lee HJ, Jun JI, Choi SG, Kim H, Chung CW, Kim IK, Park IS, Chee HJ, Kim HR, Jung YK. Intracellular cleavage of osteopontin by caspase-8 modulates hypoxia/reoxygenation cell death through p53. *Proc Natl Acad Sci U S A* 2009; 106: 15326-15331.

12. Kim, M. C., Lam, R. H., Thorsen, T., and Asada, H. H. Mathematical analysis of oxygen transfer through polydimethylsiloxane membrane between double layers of cell culture channel and gas chamber in microfluidic oxygenator. *Microfluidics and Nanofluidics* 2013, 1-12.

13. Kimura, H., Braun, R. D., Ong, E. T., Hsu, R., Secomb, T. W., Papahadjopoulos, D., and Dewhirst, M. W. Fluctuations in red cell flux in tumor microvessels can lead to transient hypoxia and reoxygenation in tumor parenchyma. *Cancer Research* 1996, 56(23), 5522-5528.

14. Oppegard SC, Nam KH, Carr JR, Skaalure SC, Eddington DT. Modulating temporal and spatial oxygenation over adherent cellular cultures. *PLoS ONE* 2009; 4: e6891.

15. Parkins CS, Dennis MF, Stratford MRL, Hill SA, Chaplin DJ. Ischemia-reperfusion injury in tumors: The role of oxygen radicals and nitric oxide. *Cancer Res* 1995; 55: 6026-6029.

16. Polinkovsky M, Gutierrez E, Levchenko A, Groisman A. Fine temporal control of the medium gas content and acidity and on-chip generation of series of oxygen concentrations for cell cultures. *Lab on a Chip* 2009; 9: 1073-1084.

17. Said HM, Katzer A, Flentje M, Vordermark D. Response of the plasma hypoxia marker osteopontin to in vitro hypoxia in human tumor cells. *Radiother Oncol* 2005; 76: 200-205.

18. Subarsky P, Hill RP. Graded hypoxia modulates the invasive potential of HT1080 fibrosarcoma and MDA MB231 carcinoma cells. *Clin Exp Metastasis* 2008; 25: 253-264

19. Vaupel P, Mayer A, Hockel M. Tumor hypoxia and malignant progression. *Methods Enzymol* 2004; 381: 335-354

20. Vaupel P, Hockel M, Mayer A. Detection and Characterization of Tumor Hypoxia Using PO2 Histography. *Antioxid Redox Signal* 2007, 9(8): 1221–1235.

21. Vaupel, P. Metabolic microenvironment of tumor cells: a key factor in malignant progression. *Exp Oncol* 2010, 32(3), 125-127.

22. Yoshikawa T, Kokura S, Oyamada H, Iinuma S, Nishimura S, Kaneko T, Naito Y, Kondo M. Antitumor effect of ischemia-reperfusion injury induced by transient embolization. *Cancer Res* 1994; 54: 5033-5035.

23. Young, E. Cells, Tissues, and Organs on Chips: Challenges and Opportunities for the Cancer Tumor Microenvironment. *Integr. Biol*.2013

24. Boyden, S. The chemotactic effect of mixtures of antibody and antigen on polymorphonuclear leucocytes. *The Journal of Experimental Medicine* 1962, 115(3), 453-466.

25. Sieuwerts, A. M., Klijn, J. G., and Foekens, J. A. Assessment of the invasive potential of human gynecological tumor cell lines with the in vitro Boyden chamber assay: influences of the ability of cells to migrate through the filter membrane. *Clinical and Experimental Metastasis* 1997, 15(1), 53-62.

26. Muir, D., Sukhu, L., Johnson, J., Lahorra, M. A., and Maria, B. L. Quantitative methods for scoring cell migration and invasion in filter-based assays. *Analytical Biochemistry* 1993, 215(1), 104-109.

27. Li, Y. H., and Zhu, C. A modified Boyden chamber assay for tumor cell transendothelial migration in vitro. *Clinical and Experimental Metastasis* 1999, 17(5), 423-429.

28. Zhong, M., Shen, Y., Zheng, Y., Joseph, T., Jackson, D., and Foster, D. A. Phospholipase D prevents apoptosis in v-Src-transformed rat fibroblasts and MDA-MB-231 breast cancer cells. *Biochemical and Biophysical Research Communications* 2008, 302(3), 615-619.